

Review

## 3-D Micro and Nano Technologies for Improvements in Electrochemical Power Devices

Sunshine Holmberg <sup>1,\*</sup>, Alexandra Perebikovskiy <sup>2,\*</sup>, Lawrence Kulinsky <sup>1</sup> and Marc Madou <sup>1,3</sup>

<sup>1</sup> Department of Mechanical and Aerospace Engineering, University of California, Irvine, 5200 Engineering Hall, Irvine, CA 92697, USA; E-Mails: lkulinsky@uci.edu (L.K.); mmadou@uci.edu (M.M.)

<sup>2</sup> Department of Physics and Astronomy, University of California, Irvine, 4129 Frederick Reines Hall, Irvine, CA 92697, USA

<sup>3</sup> Department of Biomedical Engineering, University of California, Irvine, 5200 Engineering Hall, Irvine, CA 92697, USA

\* Authors to whom correspondence should be addressed; E-Mails: sholmber@uci.edu (S.H.); aperebik@uci.edu (A.P.); Tel.: +1-310-895-5988 (S.H.); Fax: + 1-773-364-9238 (S.H.).

Received: 17 February 2014; in revised form: 27 March 2014 / Accepted: 28 March 2014 /

Published: 8 April 2014

---

**Abstract:** This review focuses on recent advances in micro- and nano-fabrication techniques and their applications to electrochemical power devices, specifically microfabricated Lithium-ion batteries, enzymatic and microbial fuel cells (biofuel cells), and dye-sensitized solar cells (DSSCs). Although the maturity of these three technologies ranges from market ready (batteries) to fundamental research (biofuel cells) to applied research (DSSCs), advances in MEMS (Micro-Electro-Mechanical Systems) and NEMS (Nano-Electro-Mechanical Systems) techniques, particularly modifications in surface area and surface chemistry, and novel genetic and molecular engineering techniques, significantly improve the electrochemical activity of these technologies across the board. For each of these three categories of power-MEMS devices the review covers: (1) The technical challenges facing the performance and fabrication of electrochemical power devices; (2) Current MEMS and NEMS techniques used to improve efficiency; and (3) Future outlook and suggested improvements of MEMS and NEMS for implementation in electrochemical power devices.

**Keywords:** power devices; biofuel cell; dye sensitized solar cell; lithium battery; electrochemistry; MEMS; nanotechnology

---

## 1. Introduction

One of the greatest challenges facing modern society is the need for low cost, smart, and sustainable power conversion and energy storage systems. Ecological concerns coupled with dwindling oil and fossil fuel supplies has led to increased interest in research in advanced energy systems [1], such as lithium ion batteries, solar cells, and fuel cells. The foundation of the research and development breakthroughs of these new power systems are the innovative materials and advanced fabrication techniques that lie at the heart of the micro- and nano-revolutions. Furthermore, the coupling of biology and machinery in advanced power sources such as biofuel cells and liquid junction solar cells requires the development and application of genetic and molecular engineering techniques for the precise control and longevity of these systems.

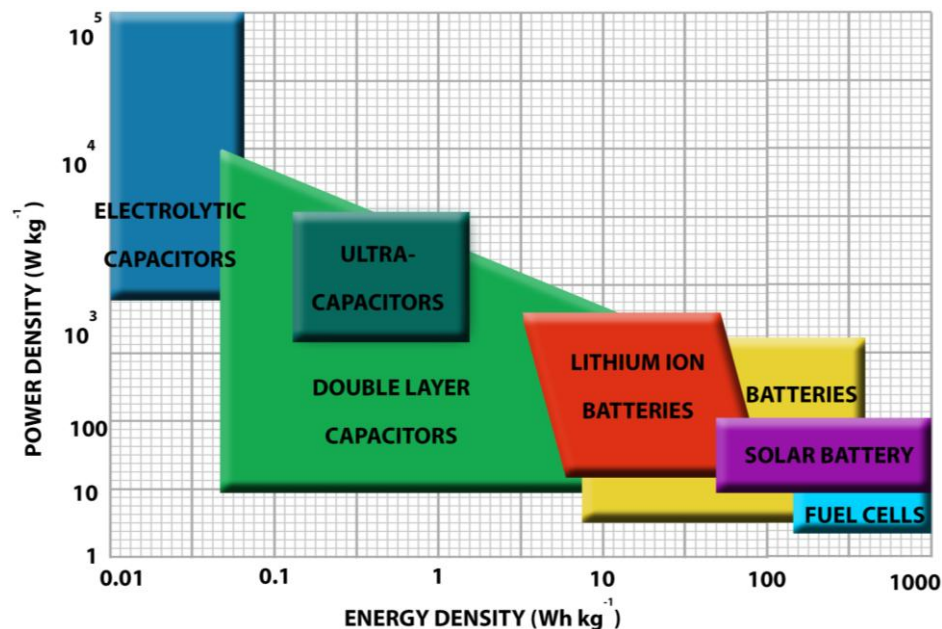
The last decade has witnessed a tremendous upsurge in nanotechnology and nanomaterials research, seeking to harness the unique catalytic effects exhibited by these materials and their enhanced surface properties [2]. Scaling laws dictate that when the dimensions of a device or its parts (such as electrodes) shrink, it leads to an increase in the surface area-to-volume ratio. This leads to an attendant increase in the amount of interfaces and increased rate of transport phenomena, such as enhanced electron transport (important for electrochemical energy conversion) or improvements in mass transport through enhanced diffusion. Nanostructures also serve as good supports for macro-sized biomolecules. Their immobilization through adsorption on to the surface of the nanoparticles mediates electron transfer processes from the biomolecule to the electrode and prevents deformation of their 3D structure and denaturing of molecules.

Electrochemistry, which underlies the energy conversion processes discussed here, is intrinsically a surface and interface science, which has seen major progress within the last few decades due in large part to the significant advances in MEMS (Micro-Electro-Mechanical Systems) and nanotechnology. As electrochemical processes are largely driven by electron exchanges between surface and solution, small changes to the surface of electrodes can greatly affect the performance and stability of electrochemical devices. For example, structured nanoelectrodes have been shown to greatly improve the mass transport of electrochemical processes, yielding electrodes with much higher current densities and sensors with much larger sensitivities [3]. Despite these breakthroughs, however, there still remain significant technical obstacles preventing the commercialization and widespread use of many advanced electrochemical MEMS- and NEMS (Nano-Electro-Mechanical Systems)-based energy and power systems.

In this review, we will focus on recent advances in MEMS and NEMS techniques and their contributions to three electrochemical power devices that are at the forefront of advanced energy research. To get a broad scope of the extent of research in this direction, we will focus our attention on devices where the utilization of new MEMS and NEMS techniques for their improvement lies at three different stages of research: Mature and commercially available lithium-ion batteries, semi-mature enzymatic, and microbial biofuel cells where nanomaterial morphologies lie in the stage of fundamental research, and dye-sensitized solar cells, where nanostructured architectures lie in the stage of applied research. Furthermore, as shown in the Ragone plot in Figure 1, we also distinguish these devices from other common power devices by focusing on devices that have higher energy density rather than power density. We will elaborate the challenges that still exist for each device, MEMS and

NEMS solutions currently being implemented, and future outlooks and applications in these advanced energy and power systems. We will also discuss the potential of utilizing dye sensitized solar cells to produce a “solar battery” that not only converts sunlight into usable energy but can also store energy as chemical potential.

**Figure 1.** Ragone Plot depicting energy vs. power densities of common power devices.



## 2. Lithium Ion Batteries

Lithium ion batteries (see Figure 2) exemplify a commercially available mature technology in the battery market, along with conventional lead acid and nickel cadmium batteries. The lithium ion battery, which typically utilizes an intercalated lithium cobalt oxide cathode, such as  $\text{LiCoO}_2$ , a carbon anode, and lithium salt electrolyte, has been an integral part of the commercial battery market for over a decade due to its high energy density (typical lithium ion batteries have a nominal voltage of 3.7 V as compared to 2 V for lead-acid batteries and 1.2 V for Nickel Cadmium batteries), little to no memory effect, and long shelf life. According to a Frost and Sullivan Report from 2013 [4], this market is expected to double by 2016 from 1.7 billion in 2012. Li-ion battery applications range from common electronic devices, such as cell phones and laptops, to larger scale applications such as electric vehicles, power tools, grid storage systems, and even the Mars Rover program.

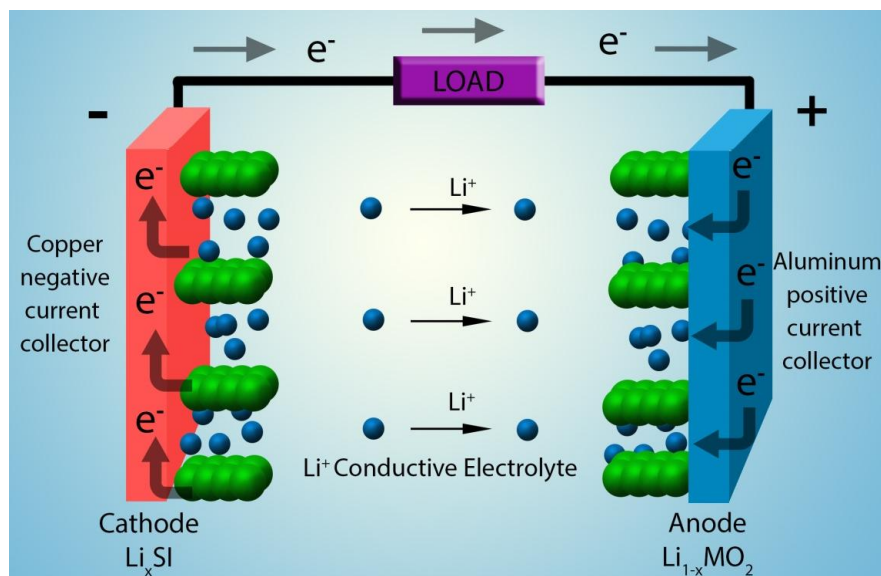
Although lithium ion batteries have been commercially used for more than two decades as a good power source for portable electronics, current electrode materials and chemistries are reaching their limits in performance and safety, particularly for emerging applications, such as electric vehicles and as energy storage systems for smart grids. Challenges include lithium dendrite formation when using lithium metals for the anode, safety concerns due to flammable electrolytes, cycle life and recharging time, cost, and materials availability. Cutting edge research is focused on improving three critical characteristics of lithium ion batteries: energy density, power density, and safety.

Although changes in battery design can help with some of these challenges, breakthroughs in battery materials are indispensable. Advances in lithium batteries can be achieved by new and

innovative nanomaterials and MEMS techniques for both the electrodes and the electrolytes for improved battery performance. While there are some disadvantages of implementing nanomaterials in lithium batteries (such as complexity of synthesis and potentially undesirable electrode and electrolyte reactions), the switch to nanomaterials and novel architectures is expected to improve lithium ion batteries in several key ways:

1. Shorter diffusion path lengths, in contact with current collectors for Li-ion transport from particle core to surface, resulting in increases in power density.
2. Higher charge/discharge rates and greater power density due to the higher surface area of the electrodes.
3. Improvements in cycle life due to decrease of mechanical stresses from lithium insertion and removal.

**Figure 2.** A typical lithium-ion battery utilizes a graphite-like anode and an intercalated lithium cobalt cathode, separated by a liquid electrolyte containing lithium ions. A lithium battery is charged by the removal of lithium ions through the oxidation of cobalt in the cathode and insertion of lithium ions into the carbon or graphite anode. As ions move from the cathode to the anode (represented by the arrows on Figure 2), cobalt is reduced, producing electricity and powering a load. The overall reaction of a Li-ion cell is  $C + LiCoO_2 \leftrightarrow LiC_6 + Li_{0.5}CoO_2$ .



### 2.1. Improvements in Energy and Power

Energy densities of lithium-ion batteries are limited due to the low energy density of the current intercalation compounds. To improve specific energy, composites of lithium metal alloys are used. Though these lithium metal composites have specific capacities that are markedly higher than conventional graphite electrodes ( $Li_{4.4}Si$  has a theoretical specific capacity of  $4200 \text{ mAh g}^{-1}$  compared with  $372 \text{ mAh g}^{-1}$  for graphite), the lithium intercalation comes with very large volume expansion and contraction due to phase transitions during charge and discharge of lithium cells, which can destroy electrodes. To combat these challenges, nanostructures have been developed for electrodes that buffer

these volume changes [5–7]. These structures involve the use of two different nanostructured materials, one that reacts with lithium, and another that acts as a confining buffer for lithium [8].

One of the approaches by researchers to solve this problem involved the development of an electrode structure based on a Tin-Carbon nanocomposite [9]. The carbon matrix not only provided the volume necessary to accommodate the contraction and expansion of the tin, but also acted as a protective shell for safe handling of the electrode. The nanocomposite electrode maintained capacity levels as high as  $500 \text{ mAh g}^{-1}$  for hundreds of cycles and showed high chemical stability, showing no changes in activity even after being exposed to open air at room temperature for over a month.

Most recently, Cui *et al.* [10] utilized a nanoparticle yolk shell design for a sulfur cathode in a rechargeable lithium-ion battery. The team surrounded a small sulfur nanoparticle with a hard protective shell of porous titanium oxide, leaving space for the sulfur to expand in the shell without breaking it, stabilizing the solid-electrolyte interphase on the surface of the shell. The cathode in the yolk shell design maintained performance and high capacity:  $\sim 1000 \text{ mAh g}^{-1}$  at 0.5 C after 1000 charge/discharge cycles and a coulombic efficiency of 98.4%.

A similar approach utilizes modifications in electrode morphologies, such as the use of different carbon composites, nanowire morphologies, and 3D porous particles, to achieve long cycle lives and improvements in energy density [11,12]. In 2013, researchers from San Diego [13] employed band gap engineering of nanowires to counter the volume expansion in lithium ion electrodes. The team coated germanium nanowires with an ultrathin silicon shell that created a chemical potential barrier for lithium ion diffusion through the nanowire. Instead, only axial lithiation and volume expansion occurred on these wires.

Improvements in power include the use of nanostructured electrode morphologies [14], such as nanoparticles, nanoalloys, and nanowires, to reduce diffusion length of lithium ions in and out of electrodes. Since the mass-transport of ions is most often the rate-determining step for the electrochemical reaction, increasing ion diffusion speeds increases the reaction rate significantly. Furthermore, the increase in surface to volume ratios created by these nanomorphologies greatly increases the electrochemical reactivity on the surface of electrodes for the same geometric surface area of electrodes. Mesoporous materials, such as  $\text{V}_2\text{O}_5$  aerogels or  $\text{Co}_3\text{O}_4$ /Carbon aerogel hybrids, have been used to enhance electrode capacities because of their high specific surface area, mesoporous structure, and good electrical conductivity [15].  $\text{Co}_3\text{O}_4$ /Carbon aerogel hybrids displayed good lithium storage performance and cycling stability, with a discharge capacity of  $779 \text{ mAh g}^{-1}$  and a charge capacity of  $774 \text{ mAh g}^{-1}$  after the 50th cycle [16].

Other advances include the use of nanoparticles such as nanosized or nanotextured titanium oxides to increase the surface area of the anode thereby increasing the area available for lithium ion storage [17]. These oxides, have a much greater insertion potential in comparison to lithium (1.2V to 2.0V), greatly increasing electrical power within the battery [18].

## 2.2. Improvements in Safety

Major efforts in safety improvements for lithium ion batteries focus on either the reduction of the specific energy of the battery or the use of multi-layer separators which do not necessitate the trade-off between safety and energy performance when reducing specific energy. Safety concerns, which arise

when using an organic carbonate solution electrolyte, are: the narrow stability domain, which prevents the use of high voltage cathodes, the high vapor pressure and flammability of electrolytes, and environmental and human health concerns.

Present safety improvement strategies include the use of electrolytes with additives to enhance the thermal stability of the battery [19,20], redox shuttles that protect the battery from overcharge [21], and lithium salts to reduce toxicity. Other approaches include utilizing solid state electrolytes or solid-liquid hybrids, rather than the current liquid electrolyte that is used. For example, researchers trapped liquid lithium ion solutions in a polymer matrix of polyacrylonitrile (PAN) or other gel type polymer to form a solid liquid hybrid [22]. Another approach uses ionic liquids (low temperature molten salts) as the electrolyte. These ionic liquids are not volatile or flammable, are very conductive, and are environmentally safe. Challenges include high production costs and cathode stability.

One of the most promising approaches is to use multi-layer separators such as those manufactured by Celgard (Charlot, NC, USA). These separators are thin porous membranes that physically separate the anode and the cathode, while facilitating ion transport through the cell. Another safety feature of these separators is an incorporated shutdown feature. The different layers have different phase transition temperatures so as the temperature of the cell increases, one of the membranes melts and fills the pores of the other membrane, shutting down the battery during unsafe conditions [23].

### 2.3. Future Outlook

The rapid development and commercialization of lithium batteries over the past two decades has poised them as advanced power sources of the future, expanding their role in diverse applications from power sources in miniature electronics, to hybrid cars, electrical energy storage systems, to pacemakers and implantable defibrillators, and aerospace. Nanomaterials will continue to play an increasingly significant role in lithium battery design. The most promising non-traditional lithium-ion chemistries that have shown potential for dramatic increases in power and energy density include lithium air batteries (Figure 3), lithium sulfur batteries (Figure 4), 3D battery designs (Figure 5), and biomimetic fractal structured electrodes.

**Figure 3.** Lithium-air battery schematic.

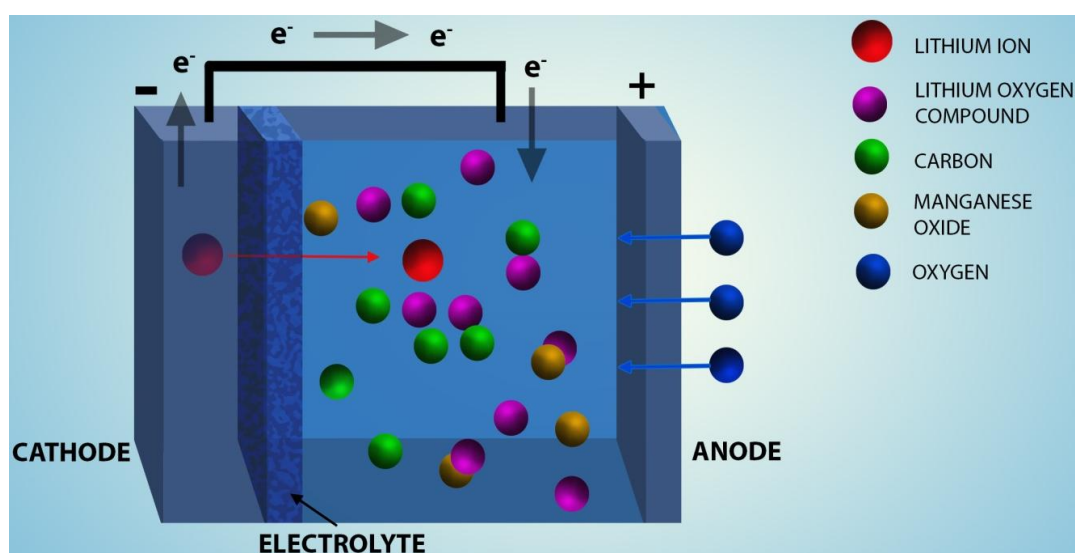




**Figure 4.** Lithium Sulfur battery schematic. The chemical reaction for the L–S battery is  $16 \text{ Li} + \text{S}_8 \leftrightarrow 8\text{Li}_2\text{S}$  and yields a theoretical energy density of  $2500 \text{ Wh kg}^{-1}$ .

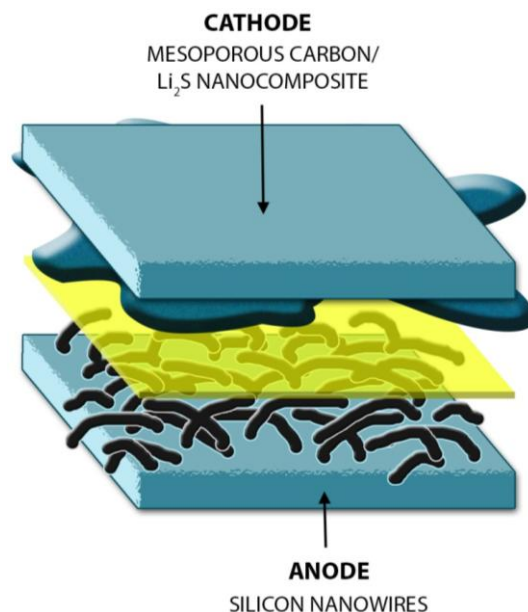
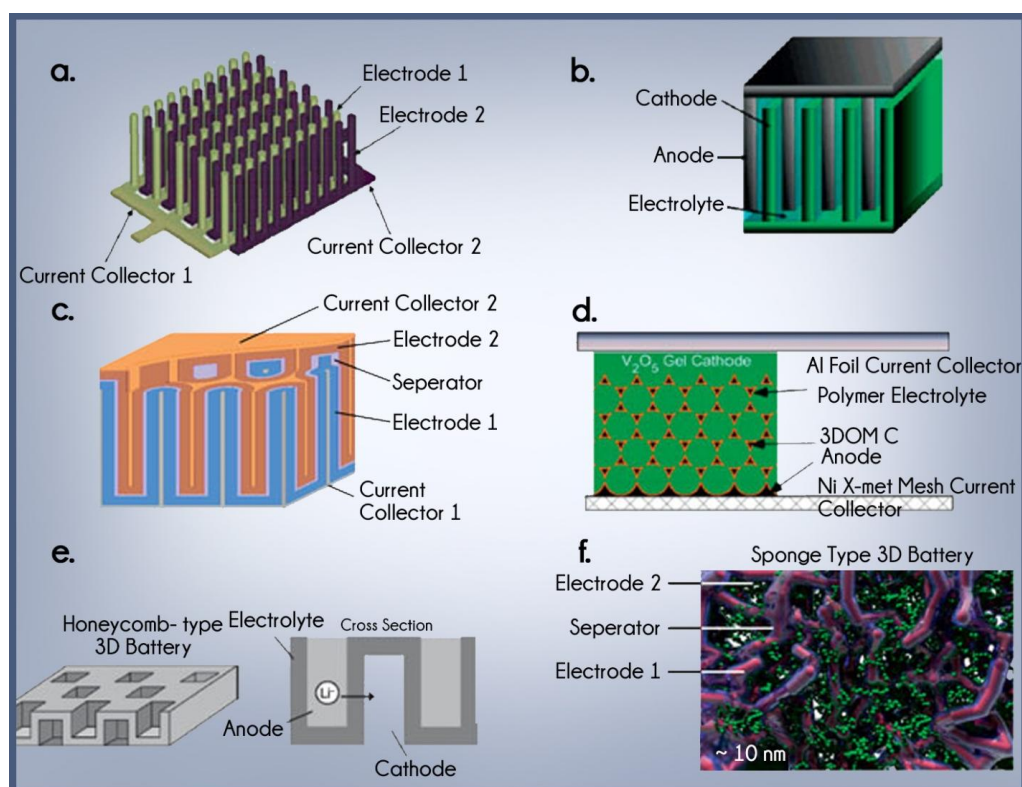


**Figure 5.** Schematic of 3D electrode architectures for 3D battery designs are shown. Adapted from reference 26. (a) interdigitated rod electrodes (©2007, IEEE) [24]; (b) interdigitated plate electrodes (©2004, American Chemical Society) [25]; (c) concentric tube design; (d) inverse opal structure based on the 3D ordered macroporous carbon (3DOM-C) structure (©2007, Electrochemical Society) [26]; (e) honeycomb-structured electrolyte (©2011, Elsevier) [27]; (f) aperiodic “sponge” design (©2007, American Chemical Society) [25].



The lithium air battery uses a lithium containing anode and a porous, carbon-based, oxygen breathing cathode. Like the high capacity, Zinc-air battery, this battery oxidizes lithium at the anode and reduces oxygen at the cathode. The theoretical energy density for lithium air, or lithium- $O_2$ , batteries is upwards of  $12 \text{ kWh kg}^{-1}$ , comparable with the energy density for gasoline ( $13 \text{ kWh kg}^{-1}$ ) and coal ( $6.7 \text{ kWh kg}^{-1}$ ). An optimization of performance of lithium-air batteries can potentially lead to power sources that can eliminate our current dependence on fossil fuels. Achieving the theoretically possible power densities of lithium air batteries requires improvements in transport of oxygen through the pores of the electrode and deposition of insulating products on active sites for oxygen reduction and evolution. Advances in nanostructures and techniques for electrode fabrication are being used to optimize lithium-air batteries. One of the most exciting advances in lithium-air batteries is IBM's announcement of the Battery 500 project. Driven by the need for long-range batteries for cars, the Battery 500 project would use a lithium air battery where the oxygen from the air would react with lithium ions during discharge, forming lithium peroxide on a carbon matrix. The oxygen would be put back in the atmosphere during recharge, when lithium is fed back into the anode [28].

The lithium-sulfur battery has a theoretical density of  $2500 \text{ Wh kg}^{-1}$  with  $500\text{--}600 \text{ Wh kg}^{-1}$  experimentally achievable. One of the main hindrances preventing commercial development of the lithium sulfur battery is the solubility of the lithium polysulfide intermediates in the battery's electrolyte solution. The polysulfides may travel through to the anode and form insolubles, hindering battery capacity and lowering the amount of usable active sulfur. Improvements have been made by using different electrolyte solutions and by using nanocomposite cathodes. Nazar *et al.* [29] used a mixture of nanostructured sulfur and mesoporous carbon to create a cathode with high charge rate capacity and reversibility.

The most promising future battery designs utilize 3-dimensional electrode architectures [30] to create a high power and high energy density battery with a small footprint. While 2D geometries can achieve large capacities, they do so mainly through increases in size, leading to bulky batteries. In addition, mechanical stress in the electrode layer increases with thickness, leading to less stable batteries. 3D electrode architectures can utilize thin film and/or nanoparticulate electrodes while decreasing the battery's footprint. For example, Nathan *et al.* [31] and Notten *et al.* [32] made a 3D substrate on glass or silicon and then deposited battery components such as electrodes and electrolyte onto the 3D structure as thin films. Other advanced battery architectures include the use of interdigitated anode/cathode rods, inverse opal structures, honeycomb-structured electrolytes and sponge-like designs (see Figure 5) which all result in higher volumetric energy densities.

The most current efforts to produce nano-fabricated electrode architectures include strategies to create and characterize the unique electrode structures involved in 3D microbatteries [33,34]. Two main structures exist. The first utilizes nanowire ( $<500 \text{ nm}$  diameter) arrays deposited directly onto a substrate acting as a current collector. The advantage of nanowire structures is in their ability to accommodate the expansion/contraction of materials without being constrained by binders or conductive additives during the fabrication process [35,36]. Electropolymerization can be utilized to electrodeposit separator layers onto them for high capacity and power density 3D miniature batteries. For example, nanowire arrays of silicon based materials have shown dramatic increases in capacity retention vs. bulk silicon [37], in major part because Si-based nanowires do not undergo the massive volume expansion upon lithiation (up to 400% in bulk Si).



Another method is used to create larger rods (>10 mm diameter) by filling a micromachined mold by electrodeposition or colloidal processing of nanoparticles. Dunn *et al.* [24,25] have utilized silicon micromachining to create an inverse template for 3D electrode array structures utilizing materials such as vanadium oxide, zinc, and mesocarbon microbeads.

A recent battery design [38] utilizes interdigitated three-dimensional bicontinuous nanoporous electrodes to create a high powered lithium-ion microbattery. The battery utilizes a porous 3-dimensional cathode and anode made by a structure of polystyrene on a glass substrate, on which nickel is electrodeposited. Then, nickel-tin is deposited onto the anode and manganese dioxide onto the cathode. Though the energy density is somewhat lower than current lithium ion batteries, the power density achieved is  $7.4 \text{ mW cm}^{-2} \mu\text{m}^{-1}$ , 2000 times higher than that of other microbatteries.

While 3D architectures yield higher energy densities in general, the challenge to small electrode area to volume ratios are that it can lead to significant resistive losses, self-discharge, and poor cycling and life times. A novel method for maximizing surface area while minimizing footprint area is inspired by nature through the use of fractal geometries to create 3D structured electrodes. Fractal electrodes maximize the effective electrode area while minimizing the resistive losses of the battery system. Fractals are utilized by nature at interfaces where matter or energy must be transferred and exchanged. For example the fractal structures observed in the capillary network in our own circulatory system utilize this unique architecture to maximize efficiency while minimizing work/energy lost [39,40]. Similar to nature, Park *et al.* [41] seek to utilize fractal networks in electrochemistry to optimize battery designs. Modeling studies of biomimetic fractal electrodes [42] show that optimizations in charging time and surface area in fractal electrodes lead to faster charging when compared to bulk electrodes and may contribute to great increases in energy and power density.

Fractal electrode geometries create an optimal electrode architecture, allowing us to maintain the high surface area of electrodes composed of nanomaterials and the thinner electrolyte use provided by using solid state electrodes [43]. Similarly, they provide an advantage over porous electrode morphologies: while porous electrodes can sometimes have closed or dead end pores which provide increases in volume with no increase in usable capacity, fractals allow a for a similar high interface area without the unusable volume.

To achieve these specific nanoarchitectures, the recent development of atomic layer deposition (ALD) shows promise as a method for engineering interfacial surfaces with sub-nm precision. ALD provides the capacity to synthesize nanomaterials and nano-architectures at the atomic level with high specificity. In lithium ion batteries, the engineering of a mere 3–4 Å layer of  $\text{Al}_2\text{O}_3$  via ALD increased the capacity retention of the  $\text{LiCoO}_2$  cathode from 45% to 90% following 120 charge/discharge cycles [44]. The ALD deposition of a 6 Å layer of  $\text{Al}_2\text{O}_3$  onto graphite anodes increased capacity retention from 26% to 96% following 200 charge/discharge cycles. Fritz *et al.* [45] hypothesized that the enhanced performance may be due to reduced corrosion, inhibition of phase changes, or reduced decomposition of the electrolyte.

### 3. Microbial and Enzymatic Biofuel Cells

Due to increased interest in alternative fuels within the last few decades, biofuel cells have become a hot topic of research and have shown great potential in certain niche markets. For example, benthic

fuel cells have been estimated to save hundreds of thousands of dollars a year in battery replacement for long term biomonitoring of water sources [46]. The term “biofuel cell” is typically used to describe either a fuel cell that uses a biological fuel or utilizes biological catalysts to convert chemical reactions to electrical work. For the purpose of this review, we will be focusing on biofuel cells that utilize biological catalysts: microbial and enzymatic biofuel cells. Microbial biofuel cells have historically been targeted towards wastewater treatment [47–49] and freshwater and seawater monitoring [50–53], though recent research has also been done on miniature microbial fuel cells for implantable biomedical devices [54,55] and other biofuel energy applications [56–58]. Enzymatic fuel cells, on the other hand, have almost exclusively been targeted toward biomedical applications—powering implantable devices [59–61]. While there has been substantial research in these two fields, innate challenges of biofuel cells have made commercialization difficult. Nanotechnology can be key in improving biofuel technology in several ways:

1. Improving power density. The similar unique dimensions of both biomolecules and nanoparticle allow us to create biomolecule nanoparticle hybrids with higher conductivity, better catalysis properties, and better electron transfer efficiencies [62,63].
2. Improving stability. Nanoparticles and nanostructures, such as solid binding matrices, provide functional and structural stability for the enzyme, creating an environment for biocatalysis [64].
3. Reducing cost. Certain nanotechnology manufacturing techniques, such as electrospinning and electropolymerization, can be used for the creation of the polymer enzyme support matrix, potentially reducing manufacturing and material costs significantly [65].

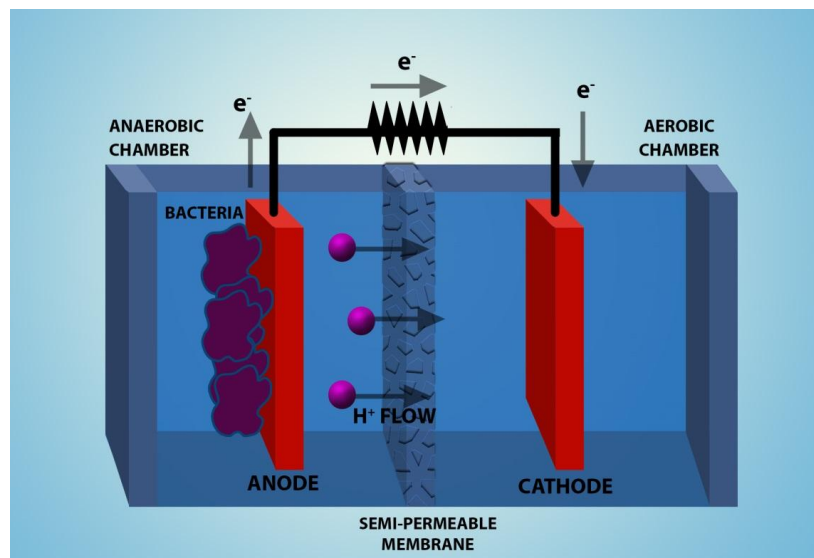
### 3.1. Microbial Fuel Cells

Ever since Potter demonstrated electron transfer between microbes and electrodes through mediator molecules in 1911 [66], there has been increasing interest in utilizing microbes in fuel cells and sensor applications. Since then, microbial fuel cells (Figure 6) have been targeted for their potential niche application in wastewater treatment and, in more recent years, implantable devices. Unfortunately, microbial fuel cells suffer from low power densities and a number of design challenges preventing commercial implementation of microbial fuel cells for wastewater treatment applications.

The main design challenge for microbial fuel cells, as they pertain to wastewater applications, is the scalability of the system in both cost and power density to meet the power needs of large-scale wastewater treatment facilities. While many of the design challenges are largely macro scale challenges, researchers have started to explore nanotechnology for means to improve the overall fuel cell efficiency. This work will focus on the research done using nanotechnology, rather than macro scale implementations.

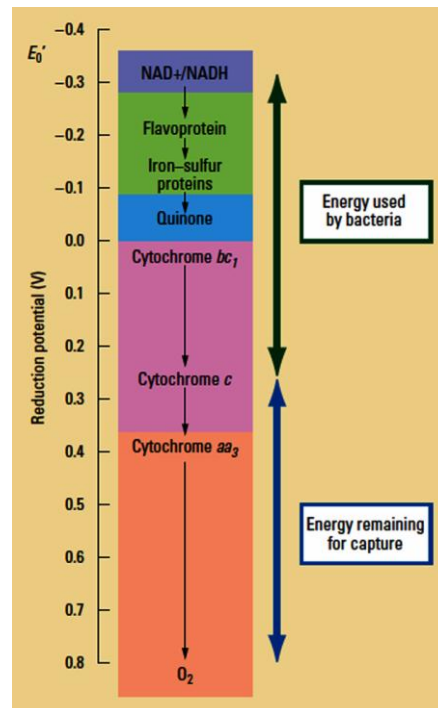
The biggest advantage of microbial fuel cells is their longevity. Microbes are robust catalysts that can extend their own lifetimes through reproduction and formation of biofilms [67,68]. The large energy density of microbial fuel cells is possible because these fuel cells utilize fuel sources already present in their operational environment. As such, microbial fuel cells with lifetimes greater than five years have been demonstrated [69].

**Figure 6.** Microbial fuel cell schematic. Microbial fuel cells utilize microbes to oxidize biofuels in their environment. Electrons are then transferred to an electrode acceptor, the anode, through extracellular electron exchange process (EEE). This exchange can occur directly between the microbe and an anode, or indirectly through mediator molecules. After the electrons pass through a load, they participate in a reduction reaction (typically, the reduction of oxygen to water) at the cathode. The typical design scheme, for most microbial fuel cells is a two-compartment design, where the anode and cathode are separated with a permeable proton exchange membrane (PEM), which allows the flow of protons to the cathode for reduction of oxygen. Organic matter flows into the anode compartment and oxygen into the cathode through small inlets to keep the electrodes in their desired working environment. A single compartment design is also possible with an open-air cathode [70–72].



The biggest limitation for microbial fuel cells is their low power density, which are orders of magnitude smaller than that of their enzymatic fuel cell counterparts. The typical power density of microbial fuel cells is about  $0.1 \text{ mW cm}^{-2}$  to  $0.1 \text{ } \mu\text{W cm}^{-2}$  [73–76] and the average enzymatic fuel cell produces between  $10 \text{ mW cm}^{-2}$  to  $10 \text{ } \mu\text{W cm}^{-2}$  [77–80]. The low power densities in microbial fuel cells are a result of several factors: loss in anodic working potential due to the microbe's respiratory chain (see Figure 7) [81], ohmic loss from formation of biofilms [82], and overpotential loss from different chemical substrates [76]. Furthermore, microbial fuel cells lose efficiency when other electron acceptors, such as oxygen, nitrates, and metal cations, are present in their working environment. The presence of electron acceptors can be reduced by sequestering the anode compartment from the rest of the fuel cell system, though this can lead to macro design challenges where scalability becomes an issue.

**Figure 7.** Microbial Fuel Cell (MFC) Respiratory Chain Diagram, which shows how energy can be recovered for the fuel cell from the potential between cytochrome c and oxygen. Figure adapted from reference [67].

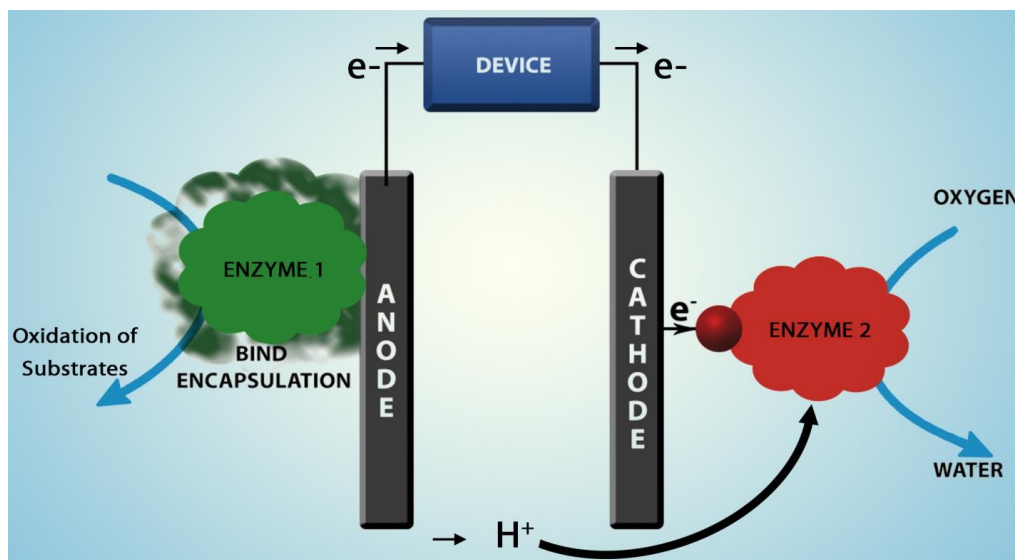


### 3.2. Enzymatic Biofuel Cells

Enzymatic fuel cells (EFCs) (see Figure 8) are attractive for powering implantable devices because their components can be made with biocompatible materials [54], they are easily integrated with MEMS devices [54,83], and they are able to employ native components of physiological fluids (*i.e.*, glucose, glycerol, *etc.*) as fuel. Due to these advantages, enzymatic fuel cells can potentially be made with little or no packaging, substantially reducing the size of many implantable devices. The biggest challenges preventing enzymatic fuel cells from commercial viability are low power densities and poor stability of the enzymes, which have short shelf and operational lifetimes. Furthermore, enzymes can be expensive and difficult to produce. Despite these challenges, researchers have continued to make incremental improvements to the efficiency and longevity of enzymatic fuel cells. Recently, Falk *et al.* [84] demonstrated the feasibility of utilizing enzymatic fuel cells for powering smart contact lenses. The fuel cell was able to produce  $1 \mu\text{W cm}^{-2}$  at 0.5 V and power their sample smart contact lenses in human lachrymal liquid, used to mimic the environment within the human eye, with a 20 h operational half-life.

Though it is inevitable that enzymes will denature over time, new and innovative immobilization schemes using both nanomorphologies and MEMS techniques show promise in improving the stability and power density of enzymatic fuel cells so that one day these “bio-batteries” can find their roles in niche applications.

**Figure 8.** Enzymatic fuel cell schematic. Enzymatic fuel cells use enzymes as the biocatalysts to oxidize organic fuels and transfer the electrons through either direct electron transfer (DET) or mediated electron transfer (MET) to the anode. DET is the process where electrons can tunnel directly from the enzyme redox centers to the electrodes. MET, on the other hand, uses mediator molecules to shuttle electrons from the enzyme to the electrode. The electrons are used to power a load and are collected at the cathode where they participate in reduction reactions. Enzymatic fuel cells have fewer design constraints than MFCs since the enzymes do not have to work in an anaerobic environment. As such, EFC's system designs do not require a separator.



### 3.3. Improvements in Power Density

One of the best, albeit most challenging, ways to improve the efficiency of fuel cells is through improvements in the performance of the biocatalyst. For example, many research groups are experimenting with mutant strains of microbes and modifying their genome in hopes of improving fuel cell efficiencies [85–88]. Yong *et al.* [86] modified the *Pseudomonas aeruginosa* microbe to overexpress NAD synthetase genes, improving the power output of the MFC threefold. Similarly, Choi *et al.* [85] modified the *Shewanella* genome by introducing glucose facilitator and glucokinase genes, increasing the range of possible substrates the microbes could oxidize. For the cathode, researchers used microbes and enzymes instead of inorganic catalysts, like platinum, due to lower overpotentials and activation losses [89–91].

EFC researchers have also utilized enzyme engineering to improve the stability and power density of EFCs. Yuhashi *et al.* [87] developed a mutant strain of pyrroloquinoline quinone modified glucose dehydrogenase (PQQGDH) that increases the stability of the enzyme by six fold and extends the lifetime to 152 h. PQQGDH is a popular enzyme utilized in both sensor and fuel cell applications due to its oxygen insensitivity, which increases the efficiency of the enzyme as a catalyst in these systems. Researchers have also utilized enzymatic cascades to mimic the processes within microbes and improve biofuel conversion efficiencies through full oxidations of biofuels that can only be partially oxidized by a single enzyme [92–94].

Ohmic losses, from high fuel cell internal resistance, can significantly reduce the power density of biofuel cells. Other factors that can contribute to the internal resistance of the cell include electrode material, electrolyte/separator material, contact resistance, and biofilm and microbe internal resistance. One solution is to utilizing noble metals for electrode materials, which can significantly reduce the internal resistance of the cell of the electrodes. Unfortunately, this method can be costly, preventing its wide scale integration.

These and similar cost constraints are the main reason carbon-based materials have become the most popular electrode support material for MFCs and EFCs. Along with its low cost, carbon has a large electrochemical stability window, biocompatibility, good conductivity, and its many allotropes all have very distinct and beneficial characteristics for electrochemical applications. Among the many carbon allotropes, carbon nanotubes (CNT) show the most promise due to their high conductivity and high aspect ratio structure, which allows them to conform to redox centers in enzymes. Mink's group [95] developed a micro MFC using a CNT anode with an air cathode and MEMS fabrication. Their MFC fabrication process is compatible with CMOS technology and utilizes biocompatible materials. The MFC developed by Mink maintained a stable high performance, at  $880 \text{ mA m}^{-2}$  and  $19 \text{ mW m}^{-2}$ , continuously for 15 days. Some of the highest power densities produced by either MFCs or EFCs have utilized CNT anodes in their electrode design [79,96,97].

Although EFC research has yielded many different electrode configuration and electrode materials, such as polymer matrices and nanoparticles, most of these systems produce substantially lower power density than carbon nanotube based electrode systems. Carbon nanotubes (CNT) have also been utilized in both EFCs and MFCs to facilitate Direct Electron Transfer (DET) between the electrode and enzymes or microbes. DET is extremely desirable in both microbial and enzymatic fuel cells because it eliminates the need for mediator molecules. Mediator molecules not only introduce addition overpotential losses, but also reduce the stability of the fuel cell, since most mediators have biological origins and are prone to degradation. Unfortunately, DET is not possible with all enzymes and in some cases mediated electron transfer (MET) has better electron transfer efficiencies and can produce more power [98].

Zebda *et al.* [98] demonstrated this in two separate works, where they utilized carbon nanotube matrix electrodes for their glucose biofuel cell (GBFC). The utilization of DET for the CNT matrix and the glucose oxidase (GOx) enzyme achieved a maximum output of  $1.25 \text{ mW cm}^{-2}$ . The second set of experiments by Zebda [79] used naphthoquinone as the mediator for MET in the CNT matrix and GOx, achieving the highest maximum power output reported for a GBFC to date:  $1.54 \text{ mW cm}^{-2}$ . This second GBFC was able to maintain a  $0.56 \text{ mWh cm}^{-2}$  energy density at 0.5 V during discharging and, with help of a charge pump, to improve mass transport of glucose, was able to power a small LED. While CNT based electrodes are capable of extremely high power output, CNT alone does very little to stabilize the enzyme and thus pure CNT biofuel cells suffer from poor lifetimes.

Another way to reduce ohmic losses is by increasing the conductivity of the electrolyte solution. One example is to utilize redox species, such as ferricyanide, in the electrolyte as electron acceptors instead of oxygen. The highest power density,  $4310 \text{ mW m}^{-2}$ , achieved by an MFC to date was reported by Rabaey *et al.* [99] who used a ferricyanide system with a graphite electrode and microbes optimized through an enrichment process. Unfortunately, many of these redox electrolyte systems,



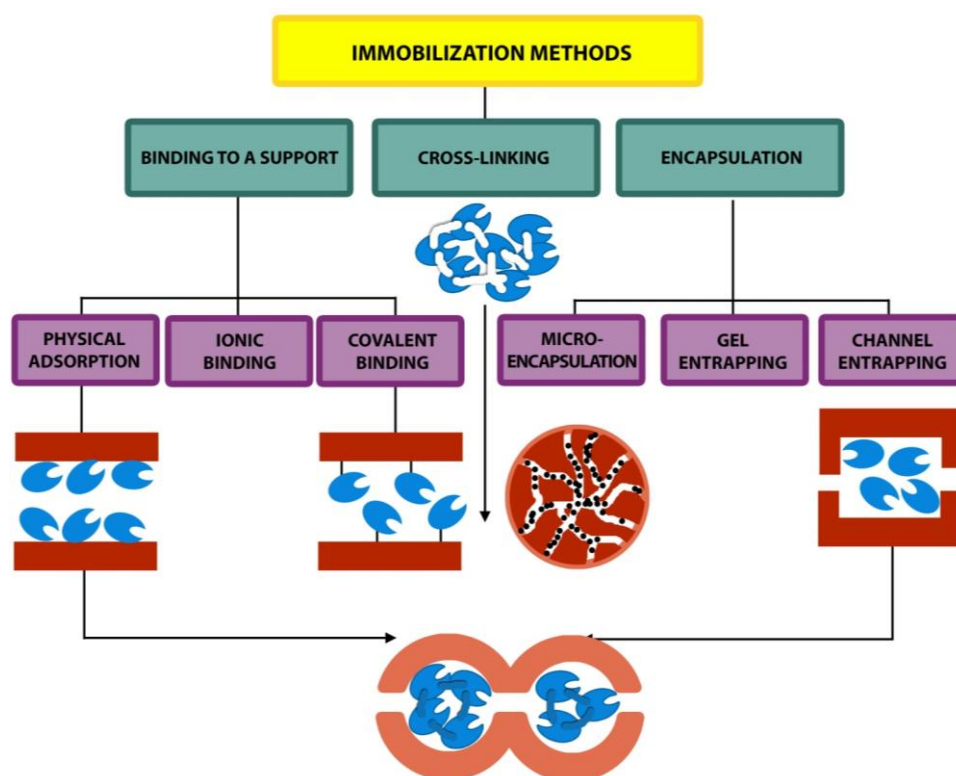
such as ferricyanide, are not feasible in most MFC applications due to the toxicity of the redox species and lack of stability (*i.e.*, the ferricyanide needs to be constantly refreshed).

### 3.4. Improvements in Stability

There are three main ways to immobilize enzymes: binding, cross-linking and encapsulation (see Figure 9). Cross-linking is the least used immobilization scheme in biofuel cells since it gives the least amount of support for the enzymes. Without incorporating other methods with cross-linking, the stability and power density is lowest for this immobilization method. Encapsulation methods, which include electropolymerization and sol-gel matrix encapsulation and entrapment, typically grant high enzyme stability, but sacrifice some catalytic ability and also exhibit mass transport limitations. Recently, researchers have incorporated CNT and metal nanoparticles into the encapsulation technique to increase the conductivity and catalytic ability of the encapsulation methods. Binding to a support typically produces better catalytic activity but poorer stability of the enzymes as compared with encapsulation techniques. Introducing pores into the matrix can also reduce mass transport problems.

Polymers have been an extremely popular area of materials research for EFCs because polymers can be used to stabilize enzymes, extending the lifetimes of EFCs. While most polymer matrices have low conductivity, they can be chemically modified or blended to be conductive. Conductive polymers, such as polypyrrole (PPy), have been extensively utilized in enzymatic biofuel cell research due to their conductive nature [100,101]. In recent years, researchers have started utilizing polymer biocomposites that blend polymers with other materials such as CNT and nanoparticles to increase the conductivity and biocatalytic ability of the electrode [64,102–104].

**Figure 9.** Enzyme Immobilization Methods [105]. Adapted from reference [94]. Printed with permission from Royal Society of Chemistry.



Perhaps the greatest advantage of polymers is their low cost and ease of manufacturing. Aside from standard lithography processes, polymer nanostructures can be produced cheaply through electrospinning or electropolymerization processes. Researchers have used electropolymerization to crosslink with and around enzymes, decreasing the gap between the polymer and the enzyme and increasing the efficiency of the electron tunneling process [106–108]. In some cases, this fabrication technique allows direct electron transfer between the polymer and enzyme, minimizing the complexity of the system [109,110]. Furthermore, polymerizing around the enzyme not only increases its electrical performance but also increases the lifetime of the enzymes [111,112]. By fabricating an environment that conforms to the enzyme, polymers stabilize the enzyme and keep it from denaturing. Rengeraj *et al.* [113] demonstrated the value of entrapment of enzymes in a polymer matrix in their research where they utilized an osmium-complex matrix to immobilize and entrap glucose oxidase, laccase and bilirubin oxidase. The group demonstrated that by entrapping the enzymes in a polymer matrix, the fuel cell retained 70% of its power after running continuously for 24 h, whereas enzymes immobilized with simple binding schemes, only retained 10% of their power output.

Nanoparticles, due to their small size, are extremely useful in biofuel cell applications because of their inherent biocatalytic abilities and their ability to help stabilize enzymes. The high surface free energy of nanoparticles allows them to strongly adsorb biomolecules and microbes, creating a very simple immobilization scheme that also stabilizes enzymes. Unfortunately, adsorbed biomolecules have a tendency to leech out, lowering the lifetime of the biofuel cell. Therefore, most biofuel cells that utilize nanoparticles are typically also entrapped in a 3D nanostructure or polymer matrix [114–116].

Nanoparticles immobilized in 3D nanostructures can be produced through electrodeposition [117], sol-gel derived methods [118], electrospraying [119], or adsorption methods [120]. Since biocatalysts are large macromolecules, which utilize a larger surface area than the nanoparticles themselves, nanostructure templates are used to create intricate nanostructures that nanoparticles can be adsorbed onto. Once the template is removed, the nanoparticles remain, creating larger nanostructures made of nanoparticles. These techniques maximize biocatalyst loading while maintaining the other natural advantages of using nanoparticles. Murata *et al.* [116] demonstrated these attractive features in their EFC utilizing three-dimensional gold nanoparticle electrodes. These electrodes not only produced a fructose/O<sub>2</sub> biofuel cell with very high power output, 0.66 mW cm<sup>-2</sup>, but also retained 90% of its power output after 48 h of continuous operation.

### 3.5. Future Outlooks

Researchers have been incrementally improving the performance of biofuel cells over the years. The main issues, power density and longevity, in the case of EFCs, have not been overcome yet, preventing commercialization. As researchers have already demonstrated, the solution will be a combination of multiple technologies, such as polymer biocomposites, which combine all the benefits of the stability and biocompatibility of polymers, with the conductivity and biocatalytic abilities of carbon materials and nanoparticles. Lee *et al.* [121] utilized a graphite oxide/cobalt, hydroxide/chitosan composite, which combines the high specific surface area of the graphite oxide with the redox activity of cobalt hydroxide and chitosan to immobilize and also stabilizes enzymes. Similarly, Deng *et al.* [122] utilized CNT/poly-L-lysine/laccase composite for Glucose EFCs, using

CNT to enable DET and poly-L-lysine for entrapment and stability of the enzymes. The maximum power density achieved by these two groups was  $517 \mu\text{W cm}^{-2}$  and  $329 \mu\text{W cm}^{-2}$ , respectively.

Polymer composites are also inexpensive and can easily be scaled for mass manufacturing techniques, such as electropolymerization and electrospinning. Electropolymerization in particular is ideal since nanoparticles and enzymes could be incorporated into the polymerization process to create a support system for enzymes that not only increases stability, but also increases electron exchange efficiency through intimate contact between nanoparticles and the enzyme.

Miniature MFCs, on the other hand, require a more in-depth look into the biology of microbes. While progress is steadily being made through utilization of nanoparticles to increase power density, the ultimate limiting factor is the microbes themselves. Genetic engineering has already proven to have a tremendous effect on improving the efficiency of MFCs and will remain a key component in incremental improvements in their performance.

Ultimately, for both MFCs and EFCs, the biggest challenge for commercialization is reassessing the advantages and constraints of these systems and determining their niche markets. While further improvements to performance will continue to push the field forward, benthic MFCs have already shown that, under the right conditions, MFCs are already commercially viable. Similarly, EFC researchers have demonstrated the feasibility of utilizing EFCs in smart contact lenses. Miniature MFCs may find success in lower power implantable sensor applications for long-term monitoring of patient vitals. Similar applications in cheap, disposable human to electronic interface devices would be the key market for EFCs. In fact, these markets may already be there, waiting for the right power source to take off.

#### 4. Dye Sensitized Solar Cells

Though the solar cell industry has been dominated by solid-state solar cells, the photoelectric experiments of Becquerel in 1839 [123], which were the original inspiration for today's photovoltaics, were done with liquid junction devices. The principle of modern solar cells utilizes the fact that at the interface between two different materials, an electric potential is created when photons strike a semiconductor surface and knock electrons out of an atom, creating electron-hole pairs. Though most solar cells utilize crystalline silicon as the bulk material, the last few decades have witnessed the development of new liquid junction solar cells with the capacity to revolutionize the photovoltaic market [124]. Ever since Dr. Michael Graetzel introduced the original concept of the Dye-Sensitized Solar Cell (DSSC) in 1988, also known as a liquid junction solar cell or Graetzel cell [125], there have been significant efforts to further research on this topic. The main attraction of DSSC technology is the low cost of materials and manufacturing processes needed to fabricate the device. The DSSC achieves this by utilizing a photosensitive dye-semiconductor interface where the excited dye injects electrons into the semiconductor. As the electrons are excited in the dye and not in the semiconductor, the charge recombination effect is avoided allowing for less purified, cheaper semiconductor materials to be used. Figure 10 illustrates the energy conversion process of DSSCs.

To date, the highest energy conversion efficiency currently obtained by DSSCs is 15% [126], up from only 1% in 1991. In order to compete commercially with current photovoltaic cells, the efficiency of DSSCs either needs to increase significantly or materials need to become cheaper. The two main

ways of increasing efficiency in DSSCs are to either extend the region of the light spectrum absorbed by the solar cell into the near infrared region to 940 nm and above [127], or to increase the open circuit voltage of the DSSC by lowering the redox potential of the electrolyte. As shown in Figure 11, several parameters needed to be engineered to improve performance: overpotentials need to be lowered and recombination rates reduced or eliminated.

**Figure 10.** The schematic of a Graetzel cell shown here converts solar radiation into electricity, imitating the natural process of photosynthesis. The steps for energy conversion are: **1.** Sunlight strikes and oxidizes dye, transferring an electron to the semiconductor. **2.** Electrons travel through the circuit and back into the solar cell. **3.** Electrons are transferred to the redox species and carried back to the oxidized dye, reducing it back to its original state. **4.** The process repeats.

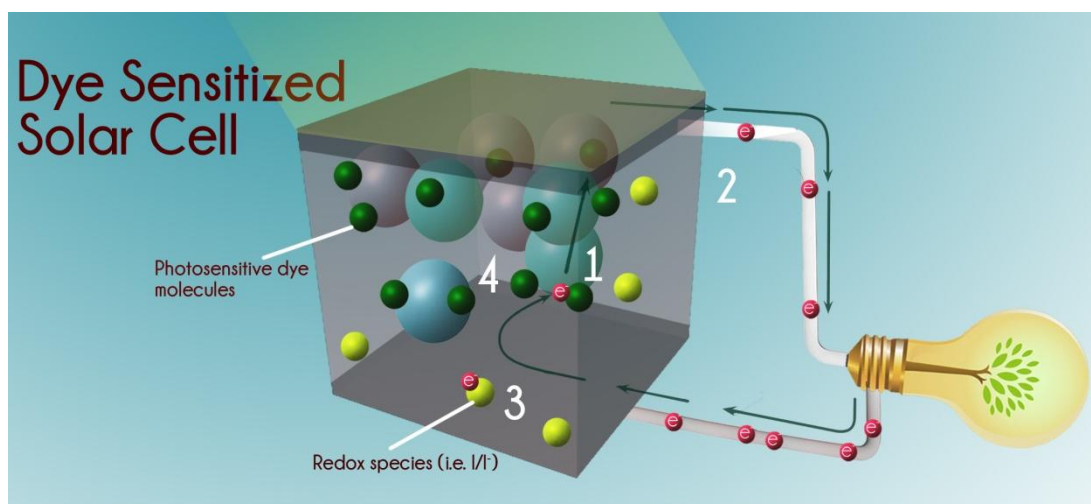
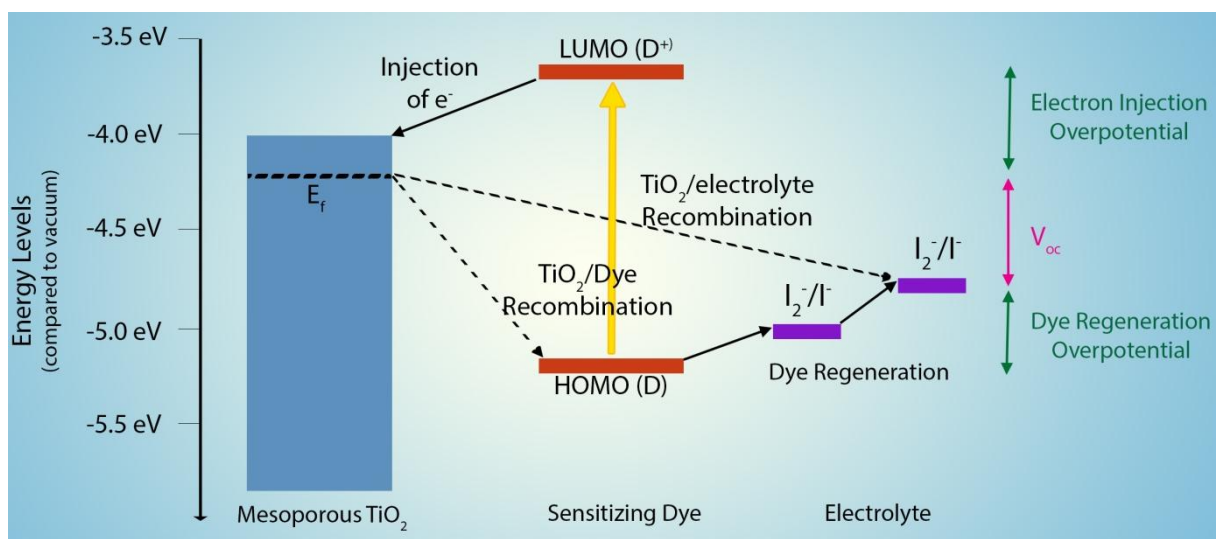


**Figure 11.** The energy band diagram illustrates the electron injection process: **(a)** Electron in the dye is excited to the energy level of the acceptor; **(b)** the acceptor energy level needs to correspond with the conduction band of the semiconductor to inject electron into the semiconductor; **(c)** the redox species in the electrolyte regenerates the dye; **(d)** redox species then regain electrons from the counter electrode [117].



#### 4.1. Challenges of Dye Sensitized Solar Cells

Unlike traditional solar cells where charge separation and transport occurs within a single medium, DSSCs convert and transport charges between multiple mediums. Due to the multi-interface system of the DSSC, DSSCs incur more overpotential losses (700 mV) than traditional solar cells, losing efficiency as charges move across different interfaces. Originally these losses were so high that the first DSSCs had an energy conversion efficiency of less than 5%. More recently new dyes and electrolytes, particularly ruthenium based complexes and  $\Gamma/\text{I}_3^-$ , and the use of perovskite-based nanomaterials, have pushed the efficiency up to 15% posing DSSCs to become competitive with conventional solar cells.

Unfortunately, there are some disadvantages associated with the utilization of these iodide and ruthenium complexes. The iodide electrolyte is very corrosive, limiting materials selection for solar cells and requiring more expensive packaging methods. Furthermore, iodide has a large overpotential due to the two-step process of regenerating the electrolyte. Ruthenium complexes utilize a rare metal making commercialization and mass production more problematic. Furthermore, these complexes do not cover the optimum spectral range—that of the near infrared (NIR) region.

Therefore, to address these and other challenges of DSSCs, future research must focus on three main challenges that exist for improvement of the efficiency of DSSCs:

1. DSSCs suffer from low open circuit voltage due to losses in potential during electron transfer from redox couples to dye molecules.
2. Only a small portion of the solar spectrum is currently absorbed by dyes, limiting the short circuit density of DSSCs. Significant increases in efficiency would require absorption in the near-infrared portion of the solar spectrum up to 940 nm.
3. Recombination losses are still significant in the titanium dioxide layer. These losses make it difficult for electrons to diffuse into the TCO substrate on the glass.

#### 4.2. Improvements in Open Circuit Voltage

The limitations of ruthenium and iodide complexes listed above have led researchers to focus on developing alternative dye/redox systems that could improve the performance of DSSCs system. For the redox couples, researchers have developed cobalt and ferrocene, as well as solid-state redox systems that use polymer based hole conductors. Cobalt and ferrocene based redox couples were able to reduce the overpotential losses, but have much faster recombination rates than iodide. Researchers have addressed this issue by modification of the titania surface with an insulating layer to prevent contact with the electrolyte solution. While this method has shown improvement in open circuit potential ( $V_{oc}$ ) it also decreases the photocurrent due to the extra insulating barrier created between the electrolyte and the titania particles.

Another extremely promising approach is to use a solid state electrolyte DSSC [128] (ssDSSCs) which modifies the ionic content of the hole conductor such that it can screen electrons from the titania and prevent recombination. Unfortunately, ssDSSCs have other problems preventing them from achieving the same efficiencies as their liquid counterpart. Some remaining obstacles for ssDSSCs are inefficient light harvesting (a wider light spectrum could be absorbed in liquid junction cells) and

lower internal quantum efficiency; ssDSSCs are also difficult to fabricate. Current techniques for fabricating hole conductors utilize solution deposition, which leaves over 50% of hole conductors porous and hollow following the evaporation step [129]. This highly porous nature creates insufficient surface coverage in ssDSSCs and results in high recombination rates and low power conversion efficiencies. However, one of the biggest breakthroughs with ssDSSCs has occurred through the use of perovskite based solar cells, increasing efficiency from 3.8% to 15% in the last four years [130]. Perovskite nanoparticles were first used as high-efficiency light sensitizers in iodide/triiodide liquid electrolyte dye solar cells. Efficiency was significantly increased by utilizing solid-state HTMs as electrolytes and through the deposition of perovskite nanocrystals onto  $\text{TiO}_2$  films [131].

#### 4.3. Light Trapping and Charge Collection Methods

Light trapping methods that increase the path length of light in the DSSC have been used extensively to increase the efficiency of DSSCs. A challenge is to design a DSSC that is thick enough to absorb all the light impinging on it, while thin enough to ensure the collection of all charge carriers. Researchers have addressed this challenge via various light trapping methods.

One method, used by Yella *et al.* [132] and others [133], scatters light using relatively large titania nanoparticles (200–400 nm) deposited onto smaller sized titania nanoparticles (20–40 nm). Since the larger particles scatter more light, they increase the photon path length in the cell. Recently, Foster *et al.* [134] used a photonic crystal based DSSC design where an array of larger  $\text{TiO}_2$  nanotubes are filled with smaller  $\text{TiO}_2$  nanoparticles and the interstitial regions between the nanotubes are filled with electrolyte to enable light-trapping. Light is focused on the interior of the nanotubes due to the dielectric contrast between the interior and exterior of the nanotubes. This cell has a higher light per volume of dye absorption than most DSSCs, improving charge collection significantly and improving solar absorption by 33%, along with improved anti-reflection, light confinement and back-reflection in the cell [134].

Similar promising approaches for improving charge collection in DSSCs includes the replacement of the disordered nanoporous  $\text{TiO}_2$  layer with various nanostructured photoelectrodes. Different nanomorphologies include the use of nanowires, branched nanowires, nanotubes, and nanoflowers, which significantly increase charge collection efficiency by decreasing the pathway for direct electron transport and reducing the recombination effect [135,136]. While charge collection is improved in these morphologies, in many cases light collection is reduced due to the lower surface area for dye absorption [137]. This problem has been addressed by researchers by utilizing high surface area nanoparticles in combination with conductive nanotube or nanowire morphologies. These DSSCs have shown significant improvements in charge collection as compared to nanostructures alone [138–140].

#### 4.4. Improvements in NIR Dyes

Dye sensitized solar cells usually contain one of two classes of dyes: metal based complexes (such as the popular ruthenium dyes) and metal free organic dyes, which are lower in cost and easier to engineer. Research for DSSCs has focused on the design and molecular engineering of NIR organic dyes that can capture the largest part of the solar energy spectrum at the cheapest possible price [141]. While researchers have developed NIR dyes with orders of magnitude better molar extinction



coefficient and lower recombination rate than their ruthenium based counterparts, they suffer from a very small absorption bandwidth, low conversion efficiency, and low operation stability due to the formation of dye aggregates on the semiconductor surface and the recombination of conduction-band electrons with triiodide [142,143]. Successful engineering modifications of dyes include electron rich sections and electron poor sections functionalized with acidic binding groups connected through a pi bridge. This configuration, along with the attachment of alkyl groups on the side of the dye as a barrier between holes in the redox couple and electrons in the titania, is optimal in preventing recombination of conduction-band electrons [141,144].

To address the issue of small bandwidth and to avoid aggregation and recombination issues, researchers have utilized both co-sensitizing dyes and energy relay dyes to broaden the bandwidth of the spectrum that can be absorbed by using multiple types of dyes [145,146]. Currently some of the highest power conversion efficiencies displayed by DSSCs have used a co-sensitizing dye scheme. The only real drawback is that not all dyes have been engineered to have low recombination rates and thus some of their potential efficiency improvements have not been achieved yet. The issue of low conversion efficiency and operation stability was addressed by Kim *et al.* [147] who engineered dyes containing dimethylfluorenyl, and amorphous non-planar geometry that prevents aggregation via molecular stacking and does not degrade when exposed to light or high temperatures.

Further work to reduce charge recombination and increase the electron injection efficiency of DSSCs was done by Meier *et al.* [148] in synthesizing organic dyes with dendritic triphenylamine moieties (T1–3). Structural modifications, such as a bent conformation and a steric hindrance, yielded dyes that enabled a light-to-electricity conversion efficiency of 5.87% with  $J_{sc}$  of  $10.35 \text{ mA cm}^{-2}$  and a  $V_{oc}$  of 0.836 V [149]. It is clear that further work on engineering and synthesis of organic dyes needs to be done to yield efficiencies above 15%.

#### 4.5. Future Outlook

Aside from synthesizing better dyes and redox species, improved MEMS techniques and nanostructures are the next logical step for improving the performance of DSSCs. Recombination between the semiconductor and dye and semiconductor and redox species are major issues that can be remedied by decreasing the thickness of the semiconductor.

Another unexplored area of research that could have potential benefits for DSSCs is the use of Janus nanoparticles. These are special nanoparticles whose surface has two or more different, distinct physical and chemical properties. A DSSC could utilize Janus particles (see Figures 12 and 13) with one half a metal material, and the other a semiconductor covered with photosensitive dye. The small size of Janus particles would reduce the distance electrons must travel before reaching the metal and thereby reduce the recombination effect. Unfortunately utilizing Janus particles would limit the number of dye molecule to a few per molecule, depending on the size of the Janus particles, potentially lowering the capture efficiency of the DSSCs. However, the small size of the Janus particles would improve the mass transport of the redox species to the dye, increasing the regeneration rate of the dye and potentially offsetting the lower surface area coverage. The regeneration rate of the dye could be further increased through the use of MEMS microfluidic mixers to induce convection into the system.

Another potential DSSC efficiency enhancement could come from using conductive nanostructures and chemical vapor deposition (CVD) processes to grow thin layers of high band gap semiconductors on conductive nanostructures. These nanostructures would not only have the benefits of thin semiconductors, but also have a large accessible surface area for dye attachment.

**Figure 12.** Schematic for manufacturing of janus nanoparticles via wax emulsion method: 1. Particles are mixed into wax, which is then emulsified with water 2. Since surface energy of particles is between that of the oil and water, they will adsorb onto the interface between the surfaces 3. Face of particles sticking out of wax can now be chemically modified [150].

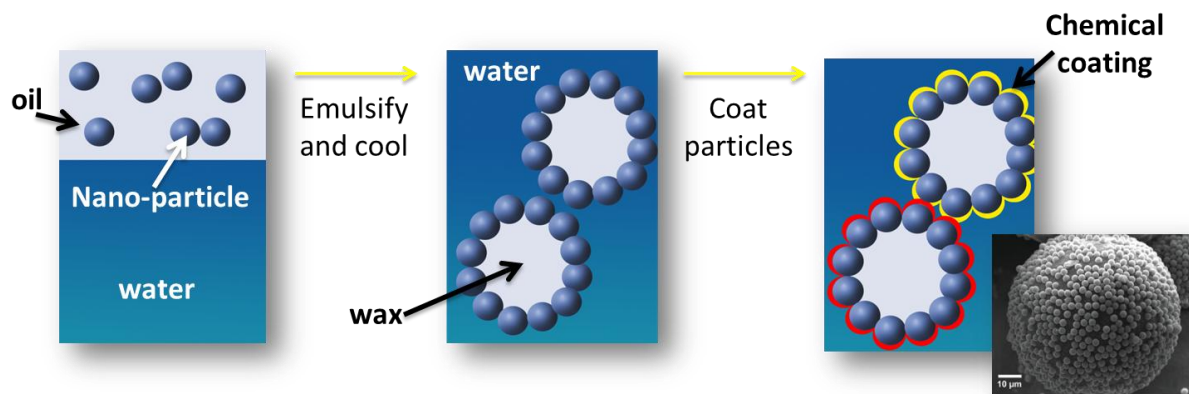
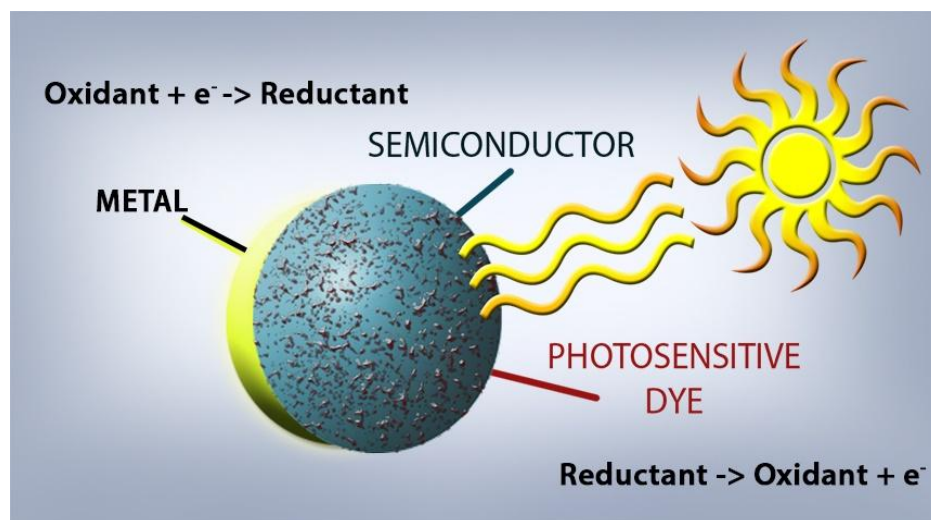


**Figure 13.** The above figure is a representation of a  $\text{TiO}_2$  Janus nanoparticle, containing a metal coating on one side and a coating of photosensitive dye on the other. As the sunlight strikes the dye and oxidizes it, an electron transfers to the semiconductor. The use of these nanoparticles lowers the distance for the electron to transfer to the metal, reducing the recombination effect.



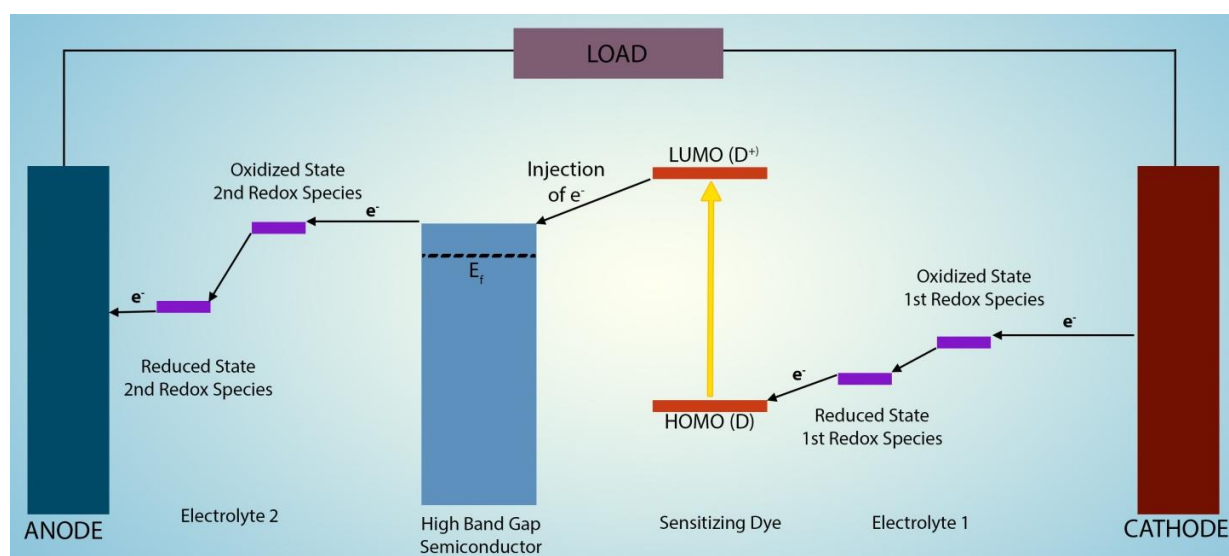
#### 4.5.1. Solar Battery

Finally, we would like to demonstrate the potential of nanotechnology through a theoretical application—the solar battery. Although there have been previous ideas for solar batteries, they are

mostly solid-state based and utilize a capacitive storage system that begins to discharge in the absence of sunlight [151,152]. The DSSC solar battery (DSSCSB) would store charge in a chemical form similar to how conventional batteries store charge.

The DSSCSB would utilize the semiconductor layer of the DSSC solar cell as a separator between two electrolyte solutions, each with its own redox system. On one side of the separator, the system behaves the same way as a standard DSSC. On the other side, another redox species would be utilized to capture an electron and ferry it to the anode. The oxidized state of the second redox species should be engineered with its energy level overlapping the energy level of the conduction band and its reduced state should be engineered to be well below the conduction band to prevent recombination. In this manner, photonic energy is captured when the DSSC is not attached to an external load and stored as chemical energy that would not discharge in the absence of sunlight (see Figure 14).

**Figure 14.** Band Gap schematic for a theoretical DSSC solar battery. The arrows show the flow of electrons through the solar battery system.



The biggest advantage of this design is its flexibility. The separator can be anything from a physical separation via a semiconductor layer, to a chemical separation via the use of a hydrophobic/hydrophilic duo electrolyte system. This also means that different nanostructured separator systems can be utilized, such as the Janus nanoparticle idea outlined earlier. We envision the solar battery to have comparable energy density to that of conventional batteries, shown in the Ragone plot in Figure 1.

## 5. Conclusions

During the 1980s, studies of surfaces under high vacuum conditions led to the development of interfacial electrochemistry. The next few decades saw a tremendous revolution in nanotechnology and MEMS techniques, the advancement of which was intimately intertwined with electrochemical applications. This review shows how the use of nanoscience and MEMS technologies opens the doorway for the commercialization of advanced electrochemical power devices such as lithium batteries, biofuel cells, and dye sensitized solar cells. In many of these technologies, enhancements in design and chemistry have reached their limits and future advances require new material

morphologies. The move to nano-structured materials, shifting the sizes of the relevant interfaces into nano-scale range significantly improves electrode and electrolyte properties, enhancing energy storage, reaction rates, power density, and capacity. Additional improvements come from the utilization of specific nanostructures for light trapping in solar cells or the use of intricate templated nanoparticle nanostructures for maximizing biocatalyst loading in fuel cells.

While these new techniques and morphologies push the boundaries of electrochemical power devices, they also present new unique challenges to scientists and researchers necessitating the development of new theories and ideas in materials chemistry and electrochemical surface science. Furthermore, with the advances in genetic science and genome sequencing, it is becoming imperative to use genetic engineering to create microbes and biomolecules finely tuned to meet the demands necessary for significant improvements in power density, energy density, and stability of bio-electrochemical power devices. This joined development of nanoscience and genetic engineering, particularly in their applications to electrochemical power devices, holds a great promise to help society meet the energy challenges of the present century.

## Acknowledgments

The authors would like to acknowledge Genis Turon Tiexidor of Enevate for his contributions to and review of the manuscript.

## Author Contributions

All authors helped conceive the idea. Sunshine Holmberg and Alexandra Perebikovsky conducted research and prepared the manuscript. Lawrence Kulinsky and Marc Madou revised the article critically for important intellectual content.

## Conflicts of Interest

The authors declare no conflict of interest.

## References

1. Markets and Market. *Advanced Energy Storage Systems Market by Technology (Pumped Hydro, Compressed Air, Batteries, Flywheels, Supercapacitors), By Applications (Grid Storage & Transportation), & Geography—Global Trends & Forecast to 2018*; Market Research Report; Markets and Market: Pune, MH, India, 2013.
2. Murty, B.; Shankar, P.; Raj, B.; Rath, B.; Murday, J. *Textbook of Nanoscience and Nanotechnology*; Springer Berlin-Heidelberg: Berlin, Germany, 2013.
3. Chen, S.; Liu, Y. Electrochemistry at nanometer-sized electrodes. *Phys. Chem. Chem. Phys.* **2014**, *16*, 635–652.
4. *Global Lithium-ion Market to Double Despite Recent Issues*; Market Research Report; Frost and Sullivan: London, UK, 2013.
5. Huggins, R.; Besenhard, J. *Handbook of Battery Materials*; Wiley VCH: Weinheim, Germany, 1999.

6. Winter, M.; Besenhard, J.O. Electrochemical lithiation of tin and tin-based intermetallics and composites. *Electrochim. Acta* **1999**, *45*, 31–50.
7. Hassoun, J.; Panero, S.; Scrosati, B. Metal alloy electrode configurations for advanced Lithium-ion batteries. *Fuel Cells* **2009**, *9*, 277–283.
8. Wu, H.; Yu, G.; Pan, L.; Liu, N.; McDowell, M.T.; Bao, Z.; Cui, Y. Stable Li-ion battery anodes by *in-situ* polymerization of conducting hydrogel to conformally coat silicon nanoparticles. *Nat. Commun.* **2013**, *4*, doi:10.1038/ncomms2941.
9. Derrien, G.; Hassoun, J.; Panero, S.; Scrosati, B. Nanostructured Sn–C composite as an advanced anode material in high-performance Lithium-ion batteries. *Adv. Mater.* **2007**, *19*, 2336–2340.
10. Seh, Z.W.; Li, W.; Cha, J.J.; Zheng, G.; Yang, Y.; McDowell, M.T.; Hsu, P.-C.; Cui, Y. Sulphur–TiO<sub>2</sub> yolk–shell nanoarchitecture with internal void space for long-cycle lithium–sulphur batteries. *Nat. Commun.* **2013**, *4*, 1331; doi:10.1038/ncomms2327.
11. Kim, H.; Han, B.; Choo, J.; Cho, J. Three-dimensional porous silicon particles for use in high-performance lithium secondary batteries. *Angew. Chemie* **2008**, *120*, 10305–10308.
12. Inoue, H. High Capacity Negative Electrode Materials Next to Carbon: Nexelion. In Proceedings of the 11th International Meeting on Lithium Batteries, Biarritz, France, 18–23 June 2006.
13. Liu, Y.; Liu, X.H.; Nguyen, B.-M.; Yoo, J.; Sullivan, J.P.; Picraux, S.T.; Huang, J.Y.; Dayeh, S.A. Tailoring lithiation behavior by interface and bandgap engineering at the nanoscale. *Nano Lett.* **2013**, *13*, 4876–4883.
14. Bruce, P.G.; Scrosati, B.; Tarascon, J.M. Nanomaterials for rechargeable lithium batteries. *Angew. Chemie Int. Ed.* **2008**, *47*, 2930–2946.
15. Shen, J.; Hou, J.; Guo, Y.; Xue, H.; Wu, G.; Zhou, B. Microstructure control of RF and carbon aerogels prepared by sol-gel process. *J. Sol Gel Sci. Technol.* **2005**, *36*, 131–136.
16. Hao, F.; Zhang, Z.; Yin, L. Co<sub>3</sub>O<sub>4</sub>/carbon aerogel hybrids as anode materials for Lithium-ion batteries with enhanced electrochemical properties. *ACS Appl. Mater. Interfaces* **2013**, *5*, 8337–8344.
17. Kubiak, P.; Fröschl, T.; Hüsing, N.; Hörmann, U.; Kaiser, U.; Schiller, R.; Weiss, C.K.; Landfester, K.; Wohlfahrt-Mehrens, M. TiO<sub>2</sub> anatase nanoparticle networks: Synthesis, structure, and electrochemical performance. *Small* **2011**, *7*, 1690–1696.
18. Scrosati, B.; Garche, J. Lithium batteries: Status, prospects and future. *J. Power Sources* **2010**, *195*, 2419–2430.
19. Croce, F.; Appetecchi, G.B.; Persi, L.; Scrosati, B. Nanocomposite polymer electrolytes for lithium batteries. *Nature* **1998**, *394*, 456–458.
20. Zhang, S.S. A review on electrolyte additives for lithium-ion batteries. *J. Power Sources* **2006**, *162*, 1379–1394.
21. Zhang, L.; Zhang, Z.; Amine, K. Redox shuttles for overcharge protection of lithium-ion battery. *ECS Trans.* **2013**, *45*, 57–66.
22. Tarascon, J.-M.; Gozdz, A.S.; Schmutz, C.; Shokoohi, F.; Warren, P.C. Performance of Bellcore’s plastic rechargeable li-ion batteries. *Solid State Ion.* **1996**, *86*, 49–54.
23. Orendorff, C.J. The role of separators in lithium-ion cell safety. *Electrochem. Soc. Interface* **2012**, *21*, 61–65.

24. Chamran, F.; Yeh, Y.; Min, H.-S.; Dunn, B.; Kim, C.-J. Fabrication of high-aspect-ratio electrode arrays for three-dimensional microbatteries. *J. Microelectromechanical Syst.* **2007**, *16*, 844–852.
25. Long, J.W.; Dunn, B.; Rolison, D.R.; White, H.S. Three-dimensional battery architectures. *Chem. Rev.* **2004**, *104*, 4463–4492.
26. Ergang, N.S.; Fierke, M.A.; Wang, Z.; Smyrl, W.H.; Stein, A. Fabrication of a fully infiltrated three-dimensional solid-state interpenetrating electrochemical cell. *J. Electrochem. Soc.* **2007**, *154*, A1135–A1139.
27. Kotobuki, M.; Suzuki, Y.; Munakata, H.; Kanamura, K.; Sato, Y.; Yamamoto, K.; Yoshida, T. Effect of sol composition on solid electrode/solid electrolyte interface for all-solid-state lithium ion battery. *Electrochimica Acta* **2011**, *56*, 1023–1029.
28. Wilcke, W. The Battery 500 Project. Available online: [https://www.ibm.com/smarterplanet/us/en/smart\\_grid/article/battery500.html](https://www.ibm.com/smarterplanet/us/en/smart_grid/article/battery500.html) (accessed on 30 January 2013).
29. Ji, X.; Lee, K.T.; Nazar, L.F. A highly ordered nanostructured carbon–sulphur cathode for lithium–sulphur batteries. *Nat. Mater.* **2009**, *8*, 500–506.
30. Arthur, T.S.; Bates, D.J.; Cirigliano, N.; Johnson, D.C.; Malati, P.; Mosby, J.M.; Perre, E.; Rawls, M.T.; Prieto, A.L.; Dunn, B. Three-dimensional electrodes and battery architectures. *MRS Bull* **2011**, *36*, 523–531.
31. Nathan, M.; Golodnitsky, D.; Yufit, V.; Strauss, E.; Ripenbein, T.; Shechtman, I.; Menkin, S.; Peled, E. Three-dimensional thin-film Li-ion microbatteries for autonomous MEMS. *J. Microelectromechanical Syst.* **2005**, *14*, 879–885.
32. Notten, P.H.; Roozeboom, F.; Niessen, H.; Baggetto, L. 3-D integrated all-solid-state rechargeable batteries. *Adv. Mater.* **2007**, *19*, 4564–4567.
33. Wang, C.; Taherabadi, L.; Jia, G.; Madou, M.; Yeh, Y.; Dunn, B. C-MEMS for the manufacture of 3D microbatteries. *Electrochem. Solid State Lett.* **2004**, *7*, A435–A438.
34. Roberts, M.; Johns, P.; Owen, J.; Brandell, D.; Edstrom, K.; Enany, G.E.; Guery, C.; Golodnitsky, D.; Lacey, M.; Lecoœur, C.; *et al.* 3D lithium ion batteries—From fundamentals to fabrication. *J. Mater. Chem.* **2011**, *21*, 9876–9890.
35. Yang, Y.; Yu, G.; Cha, J.J.; Wu, H.; Vosgueritchian, M.; Yao, Y.; Bao, Z.; Cui, Y. Improving the performance of lithium-sulfur batteries by conductive polymer coating. *Acs Nano* **2011**, *5*, 9187–9193.
36. Li, W.; Zhang, Q.; Zheng, G.; Seh, Z.W.; Yao, H.; Cui, Y. Understanding the role of different conductive polymers in improving the nanostructured sulfur cathode performance. *Nano Lett.* **2013**, *13*, 5534–5540.
37. Chan, C.K.; Peng, H.; Liu, G.; McIlwrath, K.; Zhang, X.F.; Huggins, R.A.; Cui, T. High-performance lithium battery anodes using silicon nanowires. *Nat. Nanotechnol.* **2007**, *3*, 31–35.
38. Pikul, J.H.; Zhang, H.G.; Cho, J.; Braun, P.V.; King, W.P. High-power lithium ion microbatteries from interdigitated three-dimensional bicontinuous nanoporous electrodes. *Nat. Commun.* **2013**, *4*, 1732; doi:10.1038/ncomms2747.
39. Mandelbrot, B.B. *The Fractal Geometry of Nature*; Macmillan: San Francisco, CA, USA, 1983.



40. West, G.B.; Brown, J.H.; Enquist, B.J. The fourth dimension of life: Fractal geometry and allometric scaling of organisms. *Science* **1999**, *284*, 1677–1679.
41. Park, B.Y.; Zaouk, R.; Wang, C.; Madou, M.J. A case for fractal electrodes in electrochemical applications. *J. Electrochem. Soc.* **2007**, *154*, P1–P5.
42. Turon Teixidor, G.; Park, B.Y.; Mukherjee, P.P.; Kang, Q.; Madou, M.J. Modeling fractal electrodes for Li-ion batteries. *Electrochim. Acta* **2009**, *54*, 5928–5936.
43. Madou, M. *Fundamentals of Microfabrication and Nanotechnology, Three-Volume Set: From MEMS to Bio-MEMS and Bio-NEMS: Manufacturing Techniques and Applications*; CRC Press-Taylor & Francis: Boca Raton, FL, USA, 2011.
44. Jung, Y.S.; Cavanagh, A.S.; Riley, L.A.; Kang, S.-H.; Dillon, A.C.; Groner, M.D.; George, S.M.; Lee, S.-H. Ultrathin direct atomic layer deposition on composite electrodes for highly durable and safe Li-ion batteries. *Adv. Mater.* **2010**, *22*, 2172–2176.
45. Elam, J.W.; Dasgupta, N.P.; Prinz, F.B. ALD for clean energy conversion, utilization, and storage. *MRS Bull* **2011**, *36*, 899–906.
46. Guzman, J.J.; Cooke, K.G.; Gay, M.O.; Radachowsky, S.E.; Girguis, P.R.; Chiu, M.A. Benthic Microbial Fuel Cells: Long-Term Power Sources for Wireless Marine Sensor Networks. In Proceedings of the Sensors, and Command, Control, Communications, and Intelligence (C3I) Technologies for Homeland Security and Homeland Defense IX Conference, Orlando, FL, USA, 5 April 2010.
47. Ghangrekar, M.; Shinde, V. Performance of membrane-less microbial fuel cell treating wastewater and effect of electrode distance and area on electricity production. *Bioresour. Technol.* **2007**, *98*, 2879–2885.
48. Liu, H.; Ramnarayanan, R.; Logan, B.E. Production of electricity during wastewater treatment using a single chamber microbial fuel cell. *Environ. Sci. Technol.* **2004**, *38*, 2281–2285.
49. Du, Z.; Li, H.; Gu, T. A state of the art review on microbial fuel cells: A promising technology for wastewater treatment and bioenergy. *Biotechnol. Adv.* **2007**, *25*, 464–482.
50. Gong, Y.; Radachowsky, S.E.; Wolf, M.; Nielsen, M.E.; Girguis, P.R.; Reimers, C.E. Benthic microbial fuel cell as direct power source for an acoustic modem and seawater oxygen/temperature sensor system. *Environ. Sci. Technol.* **2011**, *45*, 5047–5053.
51. Tender, L.M.; Gray, S.A.; Groveman, E.; Lowy, D.A.; Kauffman, P.; Melhado, J.; Tyce, R.C.; Flynn, D.; Petrecca, R.; Dobarro, J. The first demonstration of a microbial fuel cell as a viable power supply: powering a meteorological buoy. *J. Power Sources* **2008**, *179*, 571–575.
52. Hong, S.W.; Chang, I.S.; Choi, Y.S.; Kim, B.H.; Chung, T.K. Responses from freshwater sediment during electricity generation using microbial fuel cells. *Bioprocess Biosyst. Eng.* **2009**, *32*, 389–395.
53. Rezaei, F.; Richard, T.L.; Brennan, R.A.; Logan, B.E. Substrate-enhanced microbial fuel cells for improved remote power generation from sediment-based systems. *Environ. Sci. Technol.* **2007**, *41*, 4053–4058.
54. Siu, C.-P.B.; Chiao, M. A microfabricated PDMS microbial fuel cell. *J. Microelectromechanical Syst.* **2008**, *17*, 1329–1341.
55. Chiao, M.; Lin, L.; Lam, K.-B. Implantable, Miniaturized Microbial Fuel Cell. U.S. Patent 7,160,637, 2 December 2004.

56. Watanabe, K. Recent developments in microbial fuel cell technologies for sustainable bioenergy. *J. Biosci. Bioeng.* **2008**, *106*, 528–536.
57. Ren, H.; Lee, H.-S.; Chae, J. Miniaturizing microbial fuel cells for potential portable power sources: promises and challenges. *Microfluid. Nanofluidics* **2012**, *13*, 353–381.
58. Ieropoulos, I.A.; Greenman, J.; Melhuish, C.; Horsfield, I. Microbial fuel cells for robotics: Energy autonomy through artificial symbiosis. *ChemSusChem* **2012**, *5*, 1020–1026.
59. Kerzenmacher, S.; Ducré, J.; Zengerle, R.; von Stetten, F. Energy harvesting by implantable abiotically catalyzed glucose fuel cells. *J Power Sources* **2008**, *182*, 1–17.
60. Halámková, L.; Halánek, J.; Bocharova, V.; Szczupak, A.; Alfonta, L.; Katz, E. Implanted biofuel cell operating in a living snail. *J. Am. Chem. Soc.* **2012**, *134*, 5040–5043.
61. Calabrese Barton, S.; Gallaway, J.; Atanassov, P. Enzymatic biofuel cells for implantable and microscale devices. *Chem. Rev.* **2004**, *104*, 4867–4886.
62. Willner, I.; Baron, R.; Willner, B. Integrated nanoparticle–biomolecule systems for biosensing and bioelectronics. *Biosens. Bioelectron.* **2007**, *22*, 1841–1852.
63. Habrioux, A.; Sibert, E.; Servat, K.; Vogel, W.; Kokoh, K.B.; Alonso-Vante, N. Activity of platinum-gold alloys for glucose electrooxidation in biofuel cells. *J. Phys. Chem. B* **2007**, *111*, 10329–10333.
64. Pizzariello, A.; Stred’ansky, M.; Miertuš, S. A glucose/hydrogen peroxide biofuel cell that uses oxidase and peroxidase as catalysts by composite bulk-modified bioelectrodes based on a solid binding matrix. *Bioelectrochemistry* **2002**, *56*, 99–105.
65. Wang, Z.-G.; Wan, L.-S.; Liu, Z.-M.; Huang, X.-J.; Xu, Z.-K. Enzyme immobilization on electrospun polymer nanofibers: An overview. *J. Mol. Catal. B Enzym.* **2009**, *56*, 189–195.
66. Potter, M.C. Electrical Effects Accompanying the Decomposition of Organic Compounds. In *Proceedings of the Royal Society of London. Series B, Containing Papers of a Biological Character*; The Royal Society: London, UK, 1911; Volume 84, pp. 260–276.
67. Venkata Mohan, S.; Veer Raghavulu, S.; Sarma, P. Influence of anodic biofilm growth on bioelectricity production in single chambered mediatorless microbial fuel cell using mixed anaerobic consortia. *Biosens. Bioelectron.* **2008**, *24*, 41–47.
68. Rabaey, K.; Rodriguez, J.; Blackall, L.L.; Keller, J.; Gross, P.; Batstone, D.; Verstraete, W.; Nealsen, K.H. Microbial ecology meets electrochemistry: Electricity-driven and driving communities. *ISME J.* **2007**, *1*, 9–18.
69. Kim, B.H.; Chang, I.S.; Gil, G.C.; Park, H.S.; Kim, H.J. Novel BOD (biological oxygen demand) sensor using mediator-less microbial fuel cell. *Biotechnol. Lett.* **2003**, *25*, 541–545.
70. Liu, H.; Logan, B.E. Electricity generation using an air-cathode single chamber microbial fuel cell in the presence and absence of a proton exchange membrane. *Environ. Sci. Technol.* **2004**, *38*, 4040–4046.
71. Logan, B.; Cheng, S.; Watson, V.; Estadt, G. Graphite fiber brush anodes for increased power production in air-cathode microbial fuel cells. *Environ. Sci. Technol.* **2007**, *41*, 3341–3346.
72. Clauwaert, P.; van der Ha, D.; Boon, N.; Verbeken, K.; Verhaege, M.; Rabaey, K.; Verstraete, W. Open air biocathode enables effective electricity generation with microbial fuel cells. *Environ. Sci. Technol.* **2007**, *41*, 7564–7569.

73. Ringeisen, B.R.; Henderson, E.; Wu, P.K.; Pietron, J.; Ray, R.; Little, B.; Biffinger, J.C.; Jones-Meehan, J.M. High power density from a miniature microbial fuel cell using *Shewanella oneidensis* DSP10. *Environ. Sci. Technol.* **2006**, *40*, 2629–2634.
74. Fan, Y.; Hu, H.; Liu, H. Enhanced Coulombic efficiency and power density of air-cathode microbial fuel cells with an improved cell configuration. *J. Power Sources* **2007**, *171*, 348–354.
75. Liu, H.; Cheng, S.; Logan, B.E. Power generation in fed-batch microbial fuel cells as a function of ionic strength, temperature, and reactor configuration. *Environ. Sci. Technol.* **2005**, *39*, 5488–5493.
76. Logan, B.E.; Regan, J.M. Microbial fuel cells-challenges and applications. *Environ. Sci. Technol.* **2006**, *40*, 5172–5180.
77. Palmore, G.T.R.; Bertschy, H.; Bergens, S.H.; Whitesides, G.M. A methanol/dioxygen biofuel cell that uses NAD<sup>+</sup>-dependent dehydrogenases as catalysts: Application of an electro-enzymatic method to regenerate nicotinamide adenine dinucleotide at low overpotentials. *J. Electroanal. Chem.* **1998**, *443*, 155–161.
78. Sato, F.; Togo, M.; Islam, M.K.; Matsue, T.; Kosuge, J.; Fukasaku, N.; Kurosawa, S.; Nishizawa, M. Enzyme-based glucose fuel cell using Vitamin K<sub>3</sub>-immobilized polymer as an electron mediator. *Electrochem. Commun.* **2005**, *7*, 643–647.
79. Zebda, A.; Gondran, C.; Le Goff, A.; Holzinger, M.; Cinquin, P.; Cosnier, S. Mediatorless high-power glucose biofuel cells based on compressed carbon nanotube-enzyme electrodes. *Nat. Commun.* **2011**, *2*, 370; doi:10.1038/ncomms1365.
80. Minteer, S.D.; Liaw, B.Y.; Cooney, M.J. Enzyme-based biofuel cells. *Curr. Opin. Biotechnol.* **2007**, *18*, 228–234.
81. Madigan, M.; Martinko, J.M. *Brock Biology of Microorganisms*, 11th ed.; Pearson Prentice Hall: Upper Saddle River, NJ, USA, 2006.
82. Choi, S.; Chae, J. Optimal biofilm formation and power generation in a micro-sized microbial fuel cell (MFC). *Sens. Actuators A Phys.* **2013**, *195*, 206–212.
83. Cohen, J.L.; Westly, D.A.; Pechenik, A.; Abruna, H.D. Fabrication and preliminary testing of a planar membraneless microchannel fuel cell. *J. Power Sources* **2005**, *139*, 96–105.
84. Falk, M.; Andoralov, V.; Blum, Z.; Sotres, J.; Suyatin, D.B.; Ruzgas, T.; Arnebrant, T.; Shleev, S. Biofuel cell as a power source for electronic contact lenses. *Biosens. Bioelectron.* **2012**, *37*, 38–45.
85. Choi, D.; Lee, S.B.; Kim, S.; Min, B.; Choi, I.-G.; Chang, I.S. Metabolically engineered glucose-utilizing *Shewanella* strains under anaerobic conditions. *Bioresour. Technol.* **2014**, *154*, 59–66.
86. Yong, X.-Y.; Feng, J.; Chen, Y.-L.; Shi, D.-Y.; Xu, Y.-S.; Zhou, J.; Wang, S.-Y.; Xu, L.; Yong, Y.-C.; Sun, Y.-M. Enhancement of bioelectricity generation by cofactor manipulation in microbial fuel cell. *Biosens. Bioelectron.* **2014**, *56*, 19–25.
87. Yuhashi, N.; Tomiyama, M.; Okuda, J.; Igarashi, S.; Ikebukuro, K.; Sode, K. Development of a novel glucose enzyme fuel cell system employing protein engineered PQQ glucose dehydrogenase. *Biosens. Bioelectron.* **2005**, *20*, 2145–2150.
88. Lovley, D.R. Microbial fuel cells: Novel microbial physiologies and engineering approaches. *Curr. Opin. Biotechnol.* **2006**, *17*, 327–332.

89. Rabaey, K.; Read, S.T.; Clauwaert, P.; Freguia, S.; Bond, P.L.; Blackall, L.L.; Keller, J. Cathodic oxygen reduction catalyzed by bacteria in microbial fuel cells. *ISME J.* **2008**, *2*, 519–527.
90. Barrière, F.; Ferry, Y.; Rochefort, D.; Leech, D. Targeting redox polymers as mediators for laccase oxygen reduction in a membrane-less biofuel cell. *Electrochem. Commun.* **2004**, *6*, 237–241.
91. Schaetzle, O.; Barrière, F.; Schröder, U. An improved microbial fuel cell with laccase as the oxygen reduction catalyst. *Energy Environ. Sci.* **2009**, *2*, 96–99.
92. Arechederra, R.; Minteer, S. Complete oxidation of glycerol in an enzymatic biofuel cell. *Fuel Cells* **2009**, *9*, 63–69.
93. Addo, P.K.; Arechederra, R.L.; Minteer, S.D. Evaluating enzyme cascades for methanol/air biofuel cells based on NAD<sup>+</sup>-dependent enzymes. *Electroanalysis* **2010**, *22*, 807–812.
94. Sokic-Lazic, D.; Arechederra, R.L.; Treu, B.L.; Minteer, S.D. Oxidation of biofuels: Fuel diversity and effectiveness of fuel oxidation through multiple enzyme cascades. *Electroanalysis* **2010**, *22*, 757–764.
95. Mink, J.E.; Hussain, M.M. Sustainable design of high-performance micro-sized microbial fuel cell with carbon nanotube anode and air cathode. *ACS Nano* **2013**, *7*, 6921–6927.
96. Xie, X.; Hu, L.; Pasta, M.; Wells, G.F.; Kong, D.; Criddle, C.S.; Cui, Y. Three-dimensional carbon nanotube—Textile anode for high-performance microbial fuel cells. *Nano Lett.* **2010**, *11*, 291–296.
97. Mink, J.E.; Rojas, J.P.; Logan, B.E.; Hussain, M.M. Vertically grown multiwalled carbon nanotube anode and nickel silicide integrated high performance micro-sized (1.25  $\mu$ L) microbial fuel cell. *Nano Lett.* **2012**, *12*, 791–795.
98. Reuillard, B.; Le Goff, A.; Agnès, C.; Holzinger, M.; Zebda, A.; Gondran, C.; Elouarzaki, K.; Cosnier, S. High power enzymatic biofuel cell based on naphthoquinone-mediated oxidation of glucose by glucose oxidase in a carbon nanotube 3D matrix. *Phys. Chem. Chem. Phys.* **2013**, *15*, 4892–4896.
99. Rabaey, K.; Lissens, G.; Siciliano, S.D.; Verstraete, W. A microbial fuel cell capable of converting glucose to electricity at high rate and efficiency. *Biotechnol. Lett.* **2003**, *25*, 1531–1535.
100. Qiao, Y.; Li, C.M.; Bao, S.-J.; Bao, Q.-L. Carbon nanotube/polyaniline composite as anode material for microbial fuel cells. *J. Power Sources* **2007**, *170*, 79–84.
101. Ramanavicius, A.; Habermüller, K.; Csörgi, E.; Laurinavicius, V.; Schuhmann, W. Polypyrrole-entrapped quinoxaline protein alcohol dehydrogenase. Evidence for direct electron transfer via conducting-polymer chains. *Anal. Chem.* **1999**, *71*, 3581–3586.
102. Simon, E.; Halliwell, C.M.; Toh, C.S.; Cass, A.E.; Bartlett, P.N. Immobilisation of enzymes on poly (aniline)-poly (anion) composite films. Preparation of bioanodes for biofuel cell applications. *Bioelectrochemistry* **2002**, *55*, 13–15.
103. Tarasevich, M.; Bogdanovskaya, V.; Zagudaeva, N.; Kapustin, A. Composite materials for direct bioelectrocatalysis of the hydrogen and oxygen reactions in biofuel cells. *Russ. J. Electrochem.* **2002**, *38*, 335; doi:10.1023/A:1014759529431.
104. Yehezkeli, O.; Tel-Vered, R.; Raichlin, S.; Willner, I. Nano-engineered flavin-dependent glucose dehydrogenase/gold nanoparticle-modified electrodes for glucose sensing and biofuel cell applications. *ACS Nano* **2011**, *5*, 2385–2391.

105. Hartmann, M.; Jung, D. Biocatalysis with enzymes immobilized on mesoporous hosts: the status quo and future trends. *J. Mater. Chem.* **2010**, *20*, 844–857.
106. Foulds, N.C.; Lowe, C.R. Enzyme entrapment in electrically conducting polymers. Immobilisation of glucose oxidase in polypyrrole and its application in amperometric glucose sensors. *J. Chem. Soc. Faraday Trans. 1* **1986**, *82*, 1259–1264.
107. Malitesta, C.; Palmisano, F.; Torsi, L.; Zambonin, P.G. Glucose fast-response amperometric sensor based on glucose oxidase immobilized in an electropolymerized poly (*o*-phenylenediamine) film. *Analy. Chem.* **1990**, *62*, 2735–2740.
108. Cosnier, S.; Senillou, A.; Gräzel, M.; Comte, P.; Vlachopoulos, N.; Jaffrezic Renault, N.; Martelet, C. A glucose biosensor based on enzyme entrapment within polypyrrole films electrodeposited on mesoporous titanium dioxide. *J. Electroanal. Chem.* **1999**, *469*, 176–181.
109. De Taxis Du Poet, P.; Miyamoto, S.; Murakami, T.; Kimura, J.; Karube, I. Direct electron transfer with glucose oxidase immobilized in an electropolymerized poly (*N*-methylpyrrole) film on a gold microelectrode. *Anal. Chim. Acta* **1990**, *235*, 255–263.
110. Le Goff, A.; Holzinger, M.; Cosnier, S. Enzymatic biosensors based on SWCNT-conducting polymer electrodes. *Analyst* **2011**, *136*, 1279–1287.
111. Barlett, P.; Cooper, J. A review of the immobilization of enzymes in electropolymerized films. *J. Electroanal. Chem.* **1993**, *362*, 1–12.
112. Palmisano, F.; Rizzi, R.; Centonze, D.; Zambonin, P. Simultaneous monitoring of glucose and lactate by an interference and cross-talk free dual electrode amperometric biosensor based on electropolymerized thin films. *Biosens. Bioelectron.* **2000**, *15*, 531–539.
113. Rengaraj, S.; Kavanagh, P.; Leech, D. A comparison of redox polymer and enzyme co-immobilization on carbon electrodes to provide membrane-less glucose/O<sub>2</sub> enzymatic fuel cells with improved power output and stability. *Biosens. Bioelectron.* **2011**, *30*, 294–299.
114. Hussein, L.; Urban, G.; Krüger, M. Fabrication and characterization of buckypaper-based nanostructured electrodes as a novel material for biofuel cell applications. *Phys. Chemi. Chem. Phys.* **2011**, *13*, 5831–5839.
115. Granot, E.; Katz, E.; Basnar, B.; Willner, I. Enhanced bioelectrocatalysis using Au-nanoparticle/polyaniline hybrid systems in thin films and microstructured rods assembled on electrodes. *Chem. Mater.* **2005**, *17*, 4600–4609.
116. Murata, K.; Kajiya, K.; Nakamura, N.; Ohno, H. Direct electrochemistry of bilirubin oxidase on three-dimensional gold nanoparticle electrodes and its application in a biofuel cell. *Energy Environ. Sci.* **2009**, *2*, 1280–1285.
117. Mohanty, U. Electrodeposition: A versatile and inexpensive tool for the synthesis of nanoparticles, nanorods, nanowires, and nanoclusters of metals. *J. Appl. Electrochem.* **2011**, *41*, 257–270.
118. Davis, M. Sol-Gel Derived, Porous 3D Nanostructures Designed for Applications in Energy Storage, Catalysis, and as Conductive Materials. Ph.D. Thesis, Texas Tech University, May 2013.
119. Jayasinghe, S. Electrospraying a nanoparticulate suspension. *Int. J. Nanosci.* **2006**, *5*, 35–46.
120. Lu, Z.; Yin, Y. Colloidal nanoparticle clusters: Functional materials by design. *Chem. Soc. Rev.* **2012**, *41*, 6874–6887.

121. Uk Lee, H.; Young Yoo, H.; Lkhaqvasuren, T.; Seok Song, Y.; Park, C.; Kim, J.; Wook Kim, S. Enzymatic fuel cells based on electrodeposited graphite oxide/cobalt hydroxide/chitosan composite-enzyme electrode. *Biosens. Bioelectron.* **2013**, *42*, 342–348.
122. Deng, L.; Shang, L.; Wang, Y.; Wang, T.; Chen, H.; Dong, S. Multilayer structured carbon nanotubes/poly-L-lysine/laccase composite cathode for glucose/O<sub>2</sub> biofuel cell. *Electrochem. Commun.* **2008**, *10*, 1012–1015.
123. Becquerel, A. Mémoire sur les effets électriques produits sous l'influence des rayons solaires (in French). *Comptes Rendus Séances Hebd.* **1839**, *9*, 561–567.
124. Grätzel, M. Photoelectrochemical cells. *Nature* **2001**, *414*, 338–344.
125. O'regan, B.; Grätzel, M. A low-cost, high-efficiency solar cell based on dye-sensitized. *Nature* **1991**, *353*, 737–740.
126. Ning, Z.; Fu, Y.; Tian, H. Improvement of dye-sensitized solar cells: What we know and what we need to know. *Energy Environ. Sci.* **2010**, *3*, 1170–1181.
127. Hardin, B.E.; Snaith, H.J.; McGehee, M.D. The renaissance of dye-sensitized solar cells. *Nat. Photonics* **2012**, *6*, 162–169.
128. Bach, U.; Lupo, D.; Comte, P.; Moser, J.; Weissörtel, F.; Salbeck, J.; Spreitzer, H.; Grätzel, M. Solid-state dye-sensitized mesoporous TiO<sub>2</sub> solar cells with high photon-to-electron conversion efficiencies. *Nature* **1998**, *395*, 583–585.
129. Snaith, H.J.; Humphry-Baker, R.; Chen, P.; Cesar, I.; Zakeeruddin, S.M.; Grätzel, M. Charge collection and pore filling in solid-state dye-sensitized solar cells. *Nanotechnology* **2008**, *19*, 424003; doi:10.1088/0957-4484/19/42/424003.
130. Hodes, G. Perovskite-based solar cells. *Science* **2013**, *342*, 317–318.
131. He, M.; Zheng, D.; Wang, M.; Lin, C.; Lin, Z. High efficiency perovskite solar cells: from complex nanostructure to planar heterojunction. *J. Mater. Chem. A* **2014**, *2*, 5939–6248.
132. Yella, A.; Lee, H.-W.; Tsao, H.N.; Yi, C.; Chandiran, A.K.; Nazeeruddin, M.K.; Diau, E.W.-G.; Yeh, C.-Y.; Zakeeruddin, S.M.; Grätzel, M. Porphyrin-sensitized solar cells with cobalt (II/III)-based redox electrolyte exceed 12 percent efficiency. *Science* **2011**, *334*, 629–634.
133. Palomares, E.; Clifford, J.N.; Haque, S.A.; Lutz, T.; Durrant, J.R. Control of charge recombination dynamics in dye sensitized solar cells by the use of conformally deposited metal oxide blocking layers. *J. Am. Chem. Soc.* **2003**, *125*, 475–482.
134. Foster, S.; John, S. Light-trapping in dye-sensitized solar cells. *Energy Environ. Sci.* **2013**, *6*, 2972–2983.
135. Zhang, Q.; Cao, G. Nanostructured photoelectrodes for dye-sensitized solar cells. *Nano Today* **2011**, *6*, 91–109.
136. Yu, M.; Long, Y.-Z.; Sun, B.; Fan, Z. Recent advances in solar cells based on one-dimensional nanostructure arrays. *Nanoscale* **2012**, *4*, 2783–2796.
137. Zhu, K.; Neale, N.R.; Miedaner, A.; Frank, A.J. Enhanced charge-collection efficiencies and light scattering in dye-sensitized solar cells using oriented TiO<sub>2</sub> nanotubes arrays. *Nano Lett.* **2007**, *7*, 69–74.
138. Gan, X.; Li, X.; Gao, X.; Zhuge, F.; Yu, W. ZnO nanowire/TiO<sub>2</sub> nanoparticle photoanodes prepared by the ultrasonic irradiation assisted dip-coating method. *Thin Solid Films* **2010**, *518*, 4809–4812.



139. Ku, C.-H.; Wu, J.-J. Chemical bath deposition of ZnO nanowire–nanoparticle composite electrodes for use in dye-sensitized solar cells. *Nanotechnology* **2007**, *18*, 505706; doi:10.1088/0957-4484/18/50/505706.
140. Zheng, Q.; Kang, H.; Yun, J.; Lee, J.; Park, J.H.; Baik, S. Hierarchical construction of self-standing anodized titania nanotube arrays and nanoparticles for efficient and cost-effective front-illuminated dye-sensitized solar cells. *ACS Nano* **2011**, *5*, 5088–5093.
141. Mishra, A.; Fischer, M.K.; Bäuerle, P. Metal-free organic dyes for dye-sensitized solar cells: From structure: Property relationships to design rules. *Angew. Chemie Int. Ed.* **2009**, *48*, 2474–2499.
142. Kim, D.; Lee, J.K.; Kang, S.O.; Ko, J. Molecular engineering of organic dyes containing *N*-aryl carbazole moiety for solar cell. *Tetrahedron* **2007**, *63*, 1913–1922.
143. Hagberg, D.P.; Yum, J.-H.; Lee, H.; de Angelis, F.; Marinado, T.; Karlsson, K.M.; Humphry-Baker, R.; Sun, L.; Hagfeldt, A.; Grätzel, M. Molecular engineering of organic sensitizers for dye-sensitized solar cell applications. *J. Am. Chem. Soc.* **2008**, *130*, 6259–6266.
144. Bessho, T.; Zakeeruddin, S.M.; Yeh, C.Y.; Diau, E.W.G.; Grätzel, M. Highly efficient mesoscopic dye-sensitized solar cells based on donor—Acceptor-substituted porphyrins. *Angew. Chemie Int. Ed.* **2010**, *49*, 6646–6649.
145. Hardin, B.E.; Sellinger, A.; Moehl, T.; Humphry-Baker, R.; Moser, J.-E.; Wang, P.; Zakeeruddin, S.M.; Grätzel, M.; McGehee, M.D. Energy and hole transfer between dyes attached to titania in cosensitized dye-sensitized solar cells. *J. Am. Chem. Soc.* **2011**, *133*, 10662–10667.
146. Hardin, B.E.; Hoke, E.T.; Armstrong, P.B.; Yum, J.-H.; Comte, P.; Torres, T.; Fréchet, J.M.; Nazeeruddin, M.K.; Grätzel, M.; McGehee, M.D. Increased light harvesting in dye-sensitized solar cells with energy relay dyes. *Nat. Photonics* **2009**, *3*, 406–411.
147. Kim, J.; Ko, H.M.; Cho, N.; Paek, S.; Lee, J.K.; Ko, J. Efficient small molecule organic semiconductor containing bis-dimethylfluorenyl amino benzo[*b*]thiophene for high open circuit voltage in high efficiency solution processed organic solar cell. *RSC Adv.* **2012**, *2*, 2692–2695.
148. Zang, X.-F.; Xu, Y.-F.; Iqbal, Z.; Huang, Z.-S.; Kuang, D.-B.; Wang, L.; Meier, H.; Li, Y.; Cao, D. Synthesis and photovoltaic performance of dihydrodibenzoazepine-based sensitizers with additional lateral anchor. *Dye. Pigment.* **2013**, *99*, 1072–1081.
149. Zhang, H.; Fan, J.; Iqbal, Z.; Kuang, D.-B.; Wang, L.; Cao, D.; Meier, H. Anti-recombination organic dyes containing dendritic triphenylamine moieties for high open-circuit voltage of DSSCs. *Dye. Pigment.* **2013**, *99*, 74–81.
150. Loget, G.; Kuhn, A. Bulk synthesis of Janus objects and asymmetric patchy particles. *J. Mater. Chem.* **2012**, *22*, 15457–15474.
151. Hanak, J.J. Laser Processing Technique for Fabricating Series-Connected and Tandem Junction Series-Connected Solar Cells into a Solar Battery. U.S. Patent 4,292,092, 29 September 1981.
152. Furusawa, M.; Seki, S.; Miyashita, S.; Shimoda, T.; Yudasaka, I.; Matsuki, Y.; Takeuchi, Y. Method for Manufacturing Solar Battery. U.S. Patent 6,518,087, 11 February 2003.